

Supporting Information for

Discovery of Discrete Stages in the Oxidation of Exo-Tetrahydrodicyclopentadiene (C₁₀H₁₆) Droplets Doped with Titanium-Aluminum-Boron Reactive Mixed Metal Nanopowder

Ivan Antonov,¹ Amandin Chyba,² Sahan D. Perera,¹ Andrew M. Turner,¹ Michelle L. Pantoya,³
Matthew T. Finn,⁴ Albert Epshteyn,⁴ Ralf I. Kaiser^{1*}

¹ *Department of Chemistry, University of Hawaii at Manoa, Honolulu, HI 96822*

² *Department of Applied Mathematics and Statistics, Colorado School of Mines, Golden, CO 80401*

³ *Mechanical Engineering Department, Texas Tech University, Lubbock, Texas 79409*

⁴ *U.S. Naval Research Laboratory, Washington, DC 20375*

Experimental Methods

The oxidation of exo-tetrahydrodicyclopentadiene (JP-10) droplets doped with aluminum and titanium-boron-aluminum nanoparticles was studied using the ultrasonic levitator apparatus at the University of Hawaii at Manoa. The apparatus consists of an ultrasonic levitator positioned inside a pressure-compatible process chamber. The levitator generates a 58 kHz standing sound wave oscillating between a piezoelectric transducer and a concave-shaped reflector. The sample is levitated in one of the pressure nodes of the standing wave (Supplementary Material). The droplets were injected into the levitator using a droplet deposition system consisting of a syringe, a fluid line with a feedthrough flange and needle positioned on a magnetic wobble stick. The Al-JP-10 and TiAlB-JP-10 suspensions were prepared by mixing and sonicating for 10 minutes 2 wt % of NPs with JP-10 (BOC Sciences, $\geq 98\%$) and 0.5 wt % of Span80 detergent. The Al NPs have a mean particle diameter of 96 nm with a standard deviation of 10 nm and were procured from Novacentrix (USA). The particle size distribution was measured using a dynamic light scattering (DLS) Nicomp N3000 system. The TiAlB RMNPs were prepared using a previously published procedure¹ where the material is referenced as the “Reverse Addition” sample thermally treated at 373 K under vacuum. These materials take the form of highly agglomerated nanopowders with average sizes of 400-500 nm. The levitated droplets were oblate spheroids with a volume of $4.6 \pm 2.5 \mu\text{L}$. The droplets were levitated in an atmosphere containing argon (Airgas, 99.9999%), oxygen (Airgas, 99.999%), or an oxygen-argon mixture at a total pressure 920 ± 20 Torr. After the droplet preparation, the combustion of JP-10/nanoparticle droplets was initiated with a Synrad Firestar v40 carbon dioxide (CO₂) laser and monitored with ultraviolet-visible (UV-Vis) spectroscopy and high-speed video cameras in visible and infrared (IR) light. The operation of the CO₂ laser and the detection devices was synchronized with a Quantum Composers digital delay generator. The power of the laser (32 W) was achieved at a duty cycle of 80% and a repetition rate of 1 kHz. The UV-Vis spectra were collected *in situ* in the wavelength region of 200–1100 nm using a StellarNet SILVER-Nova zAP1 UV-Vis spectrometer and a fiber optic probe. The receiving end of the probe was positioned at a distance of 12 – 32 mm from the center of the levitator. For every measurement, 127 spectra were obtained at a 1 kHz rate. The high-speed Phantom Miro Lab 3a10 video camera and FLIR A6703 IR camera operated at 1 kHz and 250 Hz rate and recorded 500 and 125 images. The triggering pulse sequence for the cameras was started at 200 ms before the CO₂ laser, while the UV-Vis spectrometer and the laser were triggered simultaneously.

Ultrasonic Levitator

The acoustic levitator is located inside a pressure-compatible process chamber (Figures S1-S2). Ultrasonic sound waves with wavelength of 5.9 mm are generated by a piezoelectric transducer operating at 58 kHz. Multiple reflections of the sound waves between the transducer and a curved reflector located about 15 mm above the transducer generate a standing wave. A micrometer manipulator is used to adjust the distance between the transducer and the reflector to an integral number of half wavelengths to achieve the resonance conditions at a given gas composition, temperature, and pressure inside the process chamber. Acoustic radiation pressure creates the axial force which allows levitating droplets with diameters smaller than the wavelength of the sound slightly below the pressure minima of the standing wave and the radial force, which centers the droplet on the levitator’s axis. The radial force is approximately one order of magnitude smaller

than the axial levitation force. The levitator is optimized to trap droplets with a mean volume of 5 μL which assume shape of oblate spheroids with mean vertical and horizontal diameters of 1.4 ± 0.2 and 2.6 ± 0.2 mm, respectively.

Deconvolution of the UV-Vis emission spectra

The UV-Vis spectra were analyzed by subtracting the broadband radiation baseline and fitting narrow atomic and molecular peaks to line shape functions or simulated spectra. The linear constrained fit was used that solves the set of equations

$$\mathbf{Ax} = \mathbf{b}$$

where \mathbf{A} is an $m \times n$ matrix, \mathbf{b} is a column vector of length m containing the emission spectrum and \mathbf{x} is the vector of length n containing fit coefficients. The n columns of the matrix \mathbf{A} were composed of simulated spectra of species identified in the data and baseline vectors for the broadband (blackbody) radiation.

All atomic lines were simulated with gaussian line shape functions placed at the line center. For selected molecular species with well-known molecular spectrum, namely OH A-X, AlO B-X, C_2 d-a, CH A-X and B-X and TiO A-X, spectral overlays were simulated using the PGopher spectral simulation program² and added to the \mathbf{A} matrix as the basis vectors. For other molecular species (BO A-X, BO_2 A-X), a PGopher simulations were used to determine the line centers of major spectral bands, and gaussian line shape functions were then added to the \mathbf{A} matrix. Constraints were placed on the values of the coefficients of the vector \mathbf{x} to ensure that $x_i > 0$ for i corresponding to the basefunctions of all species (Data S1).

To account for the baseline shape, Planck's blackbody radiation formula modified to account for the $1/\lambda$ wavelength dependence of emissivity of metal oxide nanoparticles and soot was used.

$$E(T, \lambda) = \varepsilon(T, \lambda) \frac{2\pi hc^2}{\lambda^5} \frac{1}{\exp\left(\frac{hc}{\lambda k_B T}\right) - 1} = \frac{C(T)}{\lambda^6} \left/ \left(\exp\left(\frac{hc}{\lambda k_B T}\right) - 1 \right) \right.$$

where $\varepsilon(T, \lambda)$ is emissivity, h is Planck's constant, k_B is Boltzmann's constant, c is speed of light in vacuum and $C(T)$ is a numerical fit constant that includes temperature dependence of the emissivity. Since the linear fit does not allow directly optimizing the temperature in the Planck's formula, it was fixed at $T = 2500$ K and the first and second temperature derivatives were added to \mathbf{A} . Linear combination of the Planck's function and its derivatives was sufficient to accommodate temperature variations of the shape of blackbody radiation curve within the temperature range of the experiment. In addition, slowly varying $\sin(2\pi n\lambda/\lambda_r)$ and $\cos(2\pi n\lambda/\lambda_r)$ functions were added to the baseline to accommodate for unaccounted wavelength dependencies of emitting particles. In these formulas, λ is wavelength, $\lambda_r = \lambda_{\max} - \lambda_{\min}$ is the wavelength range of the spectrum (206-1060 nm) and n are equal to $0, \pm 1, \pm 2, \dots$, typically truncated at 5. No constraints were placed on the values of x_i for the baseline functions.

The length of emission spectra m was truncated at 1700 points, whereas n was on the order of 30-40. Therefore, the set of equations was overdetermined and solved using a linear least-square optimization. The temperature was determined after the linear fit by non-linear fitting of the sum of baselines obtained in the above procedure to the modified Planck's formula in the range of wavelength 700 – 960 nm.

The above formulation of the spectral data regression provides excellent fits (Fig. S4) for spectral bands and baselines under a condition that all major spectral features are accounted for in the A matrix. The computationally efficient constrained linear least-squares fit ensures that the global solution is achieved and the fit coefficients for all species are physical, i.e., non-negative. It allows promptly (~ 1 s) extracting temporal information for the relative concentrations, temperature, and blackbody radiation intensity from large arrays (>100 of spectra) of time-resolved emission data. In principle, it is generally applicable to various types of time-resolved spectroscopy data where peak deconvolution and baseline subtraction are required. The Python source code is attached to the SI.

In addition to the linear constrained fit described above, the non-linear automated Gaussian deconvolution routine was developed. The algorithm is still in its testing phase and outputs are carefully examined. The algorithm was built with computational efficiency in mind and was coded in python³. The algorithm is described below.

The spectra are baseline corrected and then each spectrum is fitted with Gaussian functions individually. First, negative intensity values which are caused by noise or error in the baseline correction are set to zero. The spectrum is then fit by the sum of several individual Gaussian functions where every function is defined by its height, full width half maximum (FWHM), and center. A nonlinear regression approach to fit the spectrum is required to optimize all of the Gaussian function parameters (height, FWHM, center). The program uses Scipy⁴ nonlinear least_squares algorithm.

Traditionally, the spectra are manually fit is because there are many restrictions on the Gaussian functions. For this reason, the trust region reflective (TRF) least squares method as implemented in Scipy was used which performed much better in accuracy and computational time than the standard Levenberg-Marquardt (LM) method with bounds on parameters. Each spectrum may require as many as 200 parameters to optimize. This is not computationally desirable, because the convergence rate exponentially decreases with the number of fitted parameters. To circumvent this problem, the spectrum is partitioned into subsets, each subset is fit with a Gaussian model, and then the subsets are stitched back together to form a representation for the entire spectrum.

The spectrum was partitioned based on local minima in the intensity values. It was necessary to artificially reduce the intensity at the end points of each subset so that the later stitching process is more accurate. For each subset, we calculate the second derivative of the intensity values with respect to wavelength so that local minima in the second derivative represent convoluted local maxima in the original subset. The second derivative was smoothed using a rolling average to avoid maxima caused by noise in the data. Gaussian functions are initialized at each local maximum with default parameter values (height and FWHM) based on the intensity value at that maximum.

Then the leastsquares algorithm iteratively added extra Gaussian functions at subsequent steps in the locations where the residual was largest. After the Gaussian sum for each subset has been optimized, the subsets are stitched back together to form a fit for the entire original spectrum. The combined subsets are scanned for high residual and any Gaussian functions around these areas are

refit. This step was necessary because stitching the partitions back together was likely to produce error at the endpoints of each subset, even after artificially reducing the intensity near the endpoints of each subset. The result is a list of Gaussian functions that model each spectrum. An example of the automated deconvolution is presented in the Figures S5 and S6.

Source Code

```
import numpy as np

import scipy.optimize as opt

import matplotlib.pyplot as plt

import scipy.interpolate as inter

import scipy.misc as ms

gauss=lambda x,x0,A,w:A*np.exp(-0.5*((x-x0)/w)**2)/np.sqrt(2*np.pi)/w#gaussian lineshape
function

lorentz=lambda x,x0,A,w:A/np.pi/w/(1+((x-x0)/w)**2)#lorentzian lineshape function

agauss=lambda x,x0,s,w: gauss(x,x0,1e3,w/(np.exp(-s*(x-x0))+1))#asymmetric gaussian
lineshape function

BBR=lambda x,b,T: 1e45*b**2*h*c**2/x**6/(np.exp(1e9*h*c/x/kb/T)-1)#modified 1/lambda^6
Planck's function

l_bbr=lambda T,x,b:1e45*2*h*c**2*b/x**6/(np.exp(1e9*h*c/x/kb/T)-1)#formulation of
modified Planck's function for numerical evaluation of temperature derivative

class linpeak:#spectral peak class

    def __init__(self,x0,A,w,name,fun='gauss'):#initialization

        self.name=name#peak name

        self.x0=x0#peak linecenter

        self.A=A#peak area

        self.w=w#peak width

        self.fun=fun#peak lineshape function

    def val(self,x,x0=None,A=None,w=None):#evaluation of a peak at wavelength x

        if x0==None: x0=self.x0

        if A==None: A=self.A

        if w==None: w=self.w

        return self.fun(x,x0,A,w)
```

```

def der(self,x,n=1,x0=None,A=None,w=None):#evaluation of nth derivative of a peak
lineshape function

    return ms.derivative(self.val,x,dx=1e-3,n=n)

def BBR_fit(xdata,ydata,sigma,init=[1e-6,2000]):#non-linear fit of spectral data (ydata) defined
at wavelength xdata to a modified Plank's formula

fres,pcov=opt.curve_fit(BBR,xdata,ydata,sigma=sigma,absolute_sigma=True,p0=(init[0],init[1])
)

perr=np.sqrt(np.diag(pcov))

return fres,BBR(xdata,fres[0],fres[1]),perr

def dirfit(xdata,ydata,peaks,bs=0,der=0,fit_bbr=1,bg=(0,-1),NoPlot=True): #constrained linear
least-square fit of spectral data

a=np.zeros((len(xdata),(der+1)*len(peaks)+2*bs+1+int(fit_bbr)))

for i in range(der+1):

    for j in range(len(peaks)):

        a[:,j+i*len(peaks)]=peaks[j].der(xdata,n=i)

for i in range(2*bs+1):

    a[:,(der+1)*len(peaks)+i]=np.real((1j)**(-i)*np.exp(-2*np.pi*((i+1)//2)*1j*(xdata-
xdata[0])/(xdata[-1]-xdata[0]))+(-1j)**(-i)*np.exp(2*np.pi*((i+1)//2)*1j*(xdata-
xdata[0])/(xdata[-1]-xdata[0])))

for i in range(int(fit_bbr)):

    a[:, -fit_bbr+i]=ms.derivative(l_bbr,2500,n=i,args=(xdata,1e-6),order=max(3,2*i-1))

b1=np.zeros((der+1)*len(peaks)+2*bs+1+int(fit_bbr))

b2=b1+np.inf

b1[len(peaks):]=-np.inf

cov=np.linalg.inv(np.dot(a.T,a))

res=opt.lsqr_linear(a,ydata,bounds=(b1,b2))

if not NoPlot:

    plt.plot(xdata,ydata,'k')

```

```

fitres=np.zeros(len(xdata))
for i in np.arange(np.shape(a)[1]):
    fitres+=res.x[i]*a[:,i]
plt.plot(xdata,fitres,'r')
for i in range(len(peaks)):
    plotdata=np.zeros(len(xdata))
    for j in range(der+1):
        plotdata+=res.x[i+j*len(peaks)]*a[:,i+j*len(peaks)]
    plt.plot(xdata,plotdata,'g')
err=np.sqrt(np.diag(cov)*res.cost/len(xdata))
bsdata=np.zeros(len(xdata))
for i in range(2*bs+1):
    bsdata+=res.x[i+(der+1)*len(peaks)]*a[:,i+(der+1)*len(peaks)]
for i in range(int(fit_bbr)):
    bsdata+=res.x[-fit_bbr+i]*a[:, -fit_bbr+i]
if fit_bbr>0:
    try:
        fitted_BBR=BBR_fit(xdata[bg[0]:bg[1]],bsdata[bg[0]:bg[1]],sigma=np.sqrt(ydata[bg[0]:bg[1]]+
1000)/inter.splev(xdata[bg[0]:bg[1]],cs),init=[1e-6,2500])
    except:
        fitted_BBR=(0,300),[None],[0,0])
    if not NoPlot:
        plt.plot(xdata,BBR(xdata,fitted_BBR[0][0],fitted_BBR[0][1]),'b')
else:
    fitted_BBR=(0,300),[None],[0,0])
    if not NoPlot:
        plt.plot(xdata,ydata-bsdata,'purple')
return res.x*np.sum(a,axis=0),err*np.sum(a,axis=0),fitted_BBR[0::2],bsdata

```

'''

First define list of peaks, e.g. `peaks=list()`

Populate peaks with lineshape functions via `peaks.append(linpeak(x0,A,w,name,function))`

To use a spectral overlay `[ovr_x,ovr_y]`, define an interpolation function `ovr_fun(x,x0=None,A=None,w=None)`, where `x0,A,w` are dummy arguments.

Populate peaks with the function as `peaks.append(linpeak(x0,A,w,name,function=ovr_fun))` to ensure that that it return interpolated value upon `peaks[i].val(x)` call

Run the main program via

```
out = dirfit(xdata,ydata,peaks,bs=0,der=0,fit_bbr=1,bg=(1000,-250),NoPlot=True)
```

- `xdata` is the wavelengths grid,

- `ydata` is the spectral intensity

- `bs` is the number of sin, cos functions to use for the background (0 is constant offset, integer values $n > 0$ add sin and cos functions with period of

$(\lambda_{\max} - \lambda_{\min})/n$)

- `der` is the highest order of wavelength derivatives for the peaks lineshape function to use (0 - use only functions themselves, 1 - use 1st derivative, 2 - use 2nd edrivative and so on)

set `der = 0` if positions and lineshapes are well-known. Otherwise set `der = 1` to allow small corrections for `x0` position, `der = 2` to allow correcting `x0` and `w`.

Higher `der` values provide better fit but may return non-physical peaks.

- `fit_bbr` is the maximum order of Planck's function temperature derivative to use for baseline fitting

(0 - to not use the modified Plank's function, 1 - use the function itself, 2 - use the function + 1st derivative and so on)

- `bg` is the wavelength range used for the non-linear fit of the baseline to the Planck's formula for temperature determination

The function returns `out = (out[0],out[1],out[2],out[3])`

where out[0] is array containing peak areas, out[1] is 1-sigma uncertainty for out[0], out[2] is amplitude, temperature determined

in the modified Planck's formula fit and their uncertainties, out[3] is baseline obtained in the linear fit

Set NoPlot to False to enable plotting spectral data, peaks and the Planck's baseline.

'''

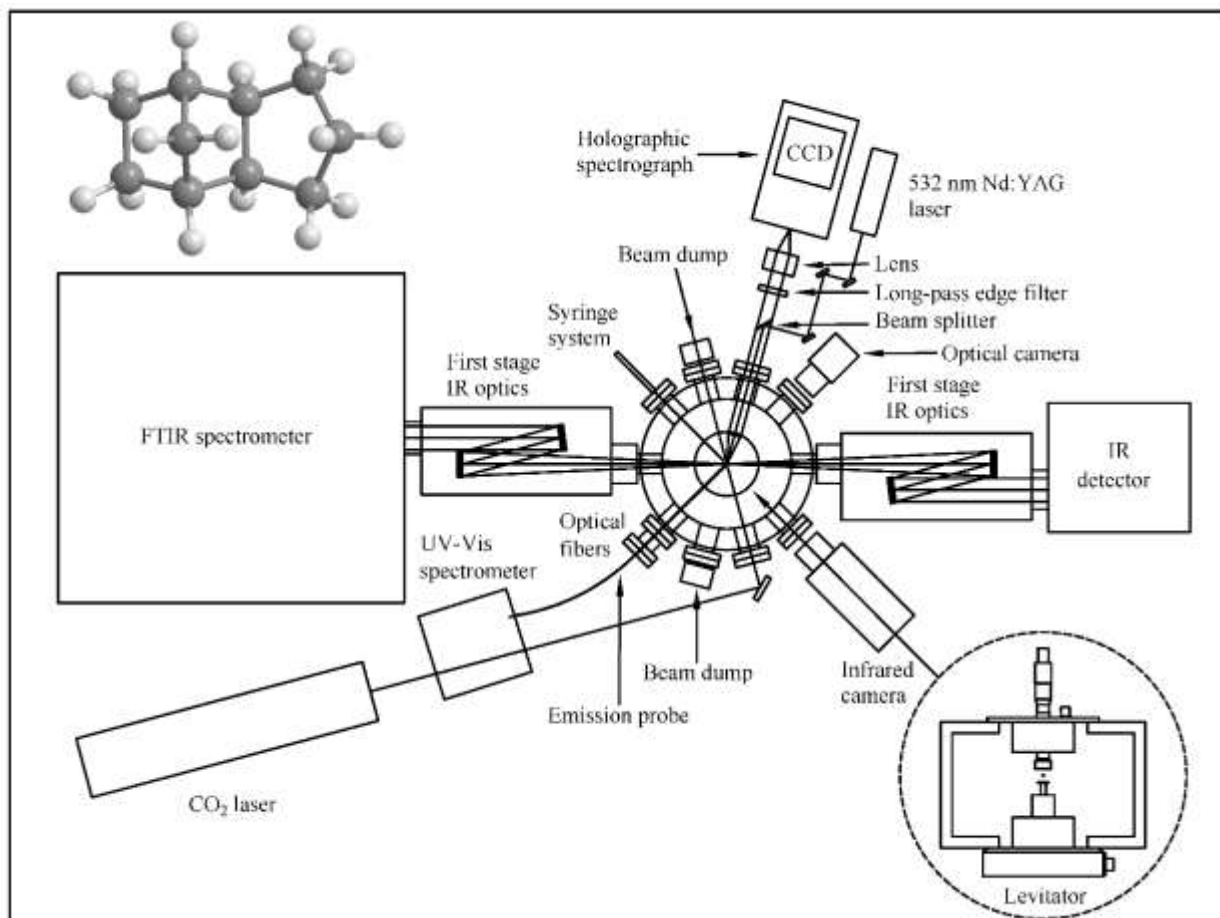


Figure S1. Schematic top view of the levitator system displaying the ultrasonic levitator, process chamber, carbon dioxide laser, Raman spectrometer, FTIR spectrometer, fiber optic UV-vis spectrometer, infrared camera, and optical camera.

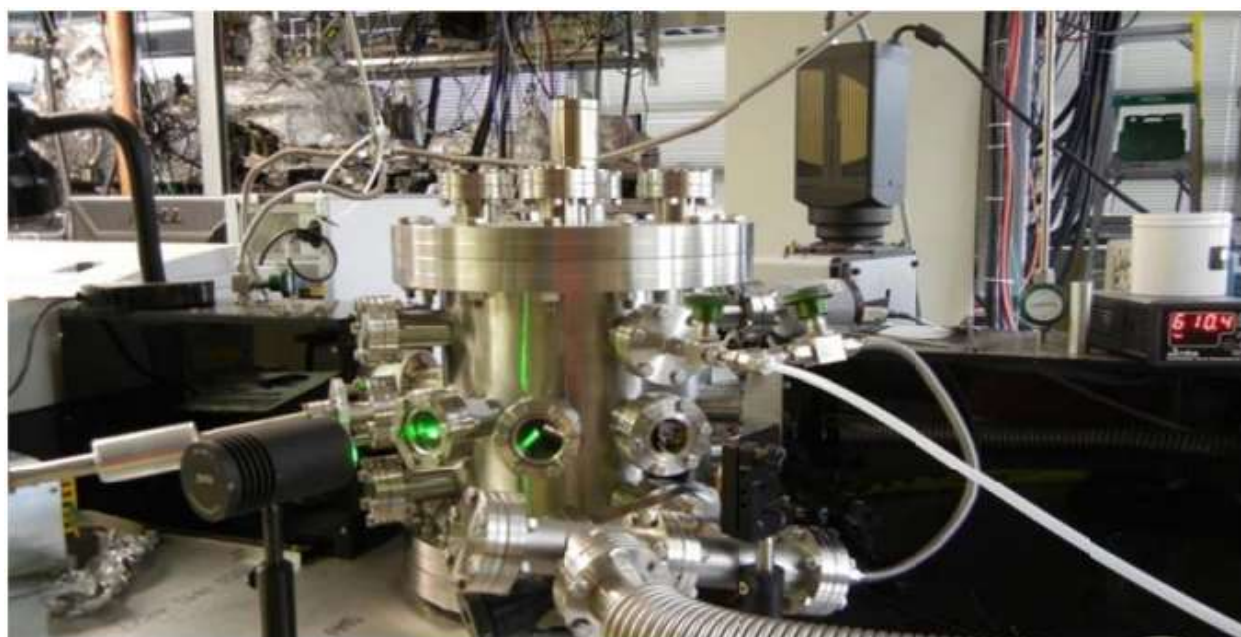


Figure S2. Photograph of the levitator.

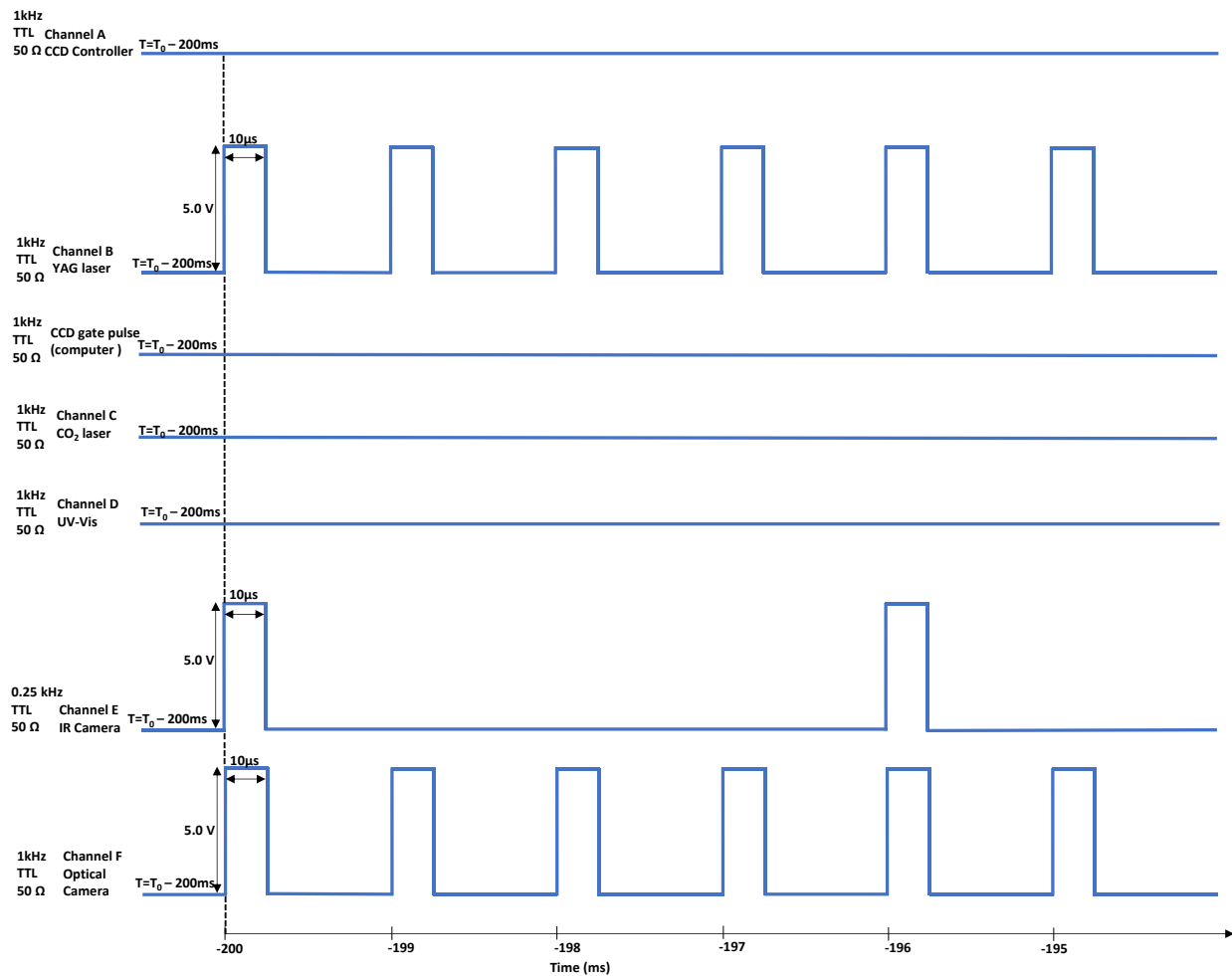


Figure S3. Pulse sequence for the experimental setup at time to collect reference spectra and reference images.

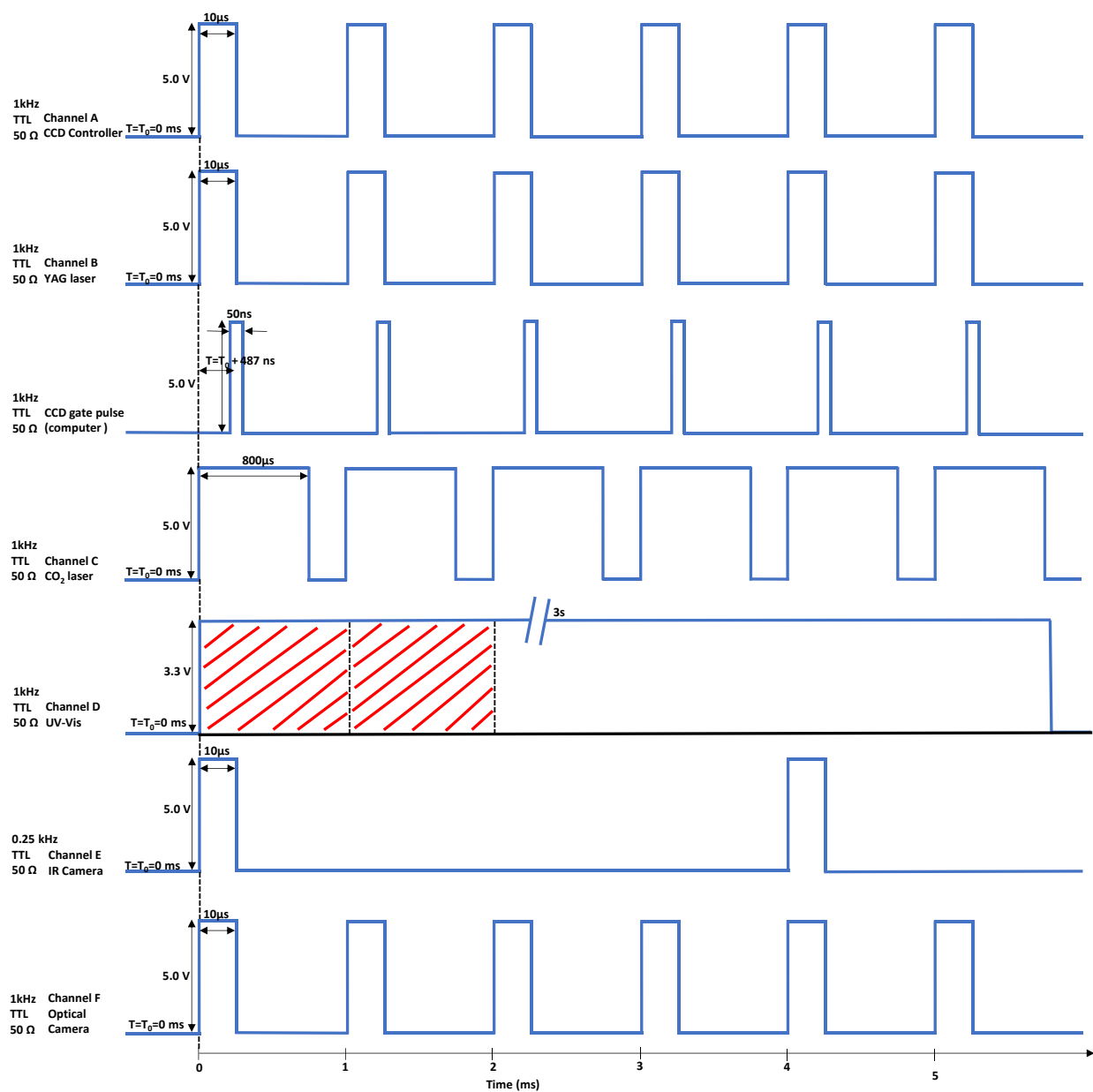


Figure S4. Pulse sequence for the present experimental setup after reference spectra have been

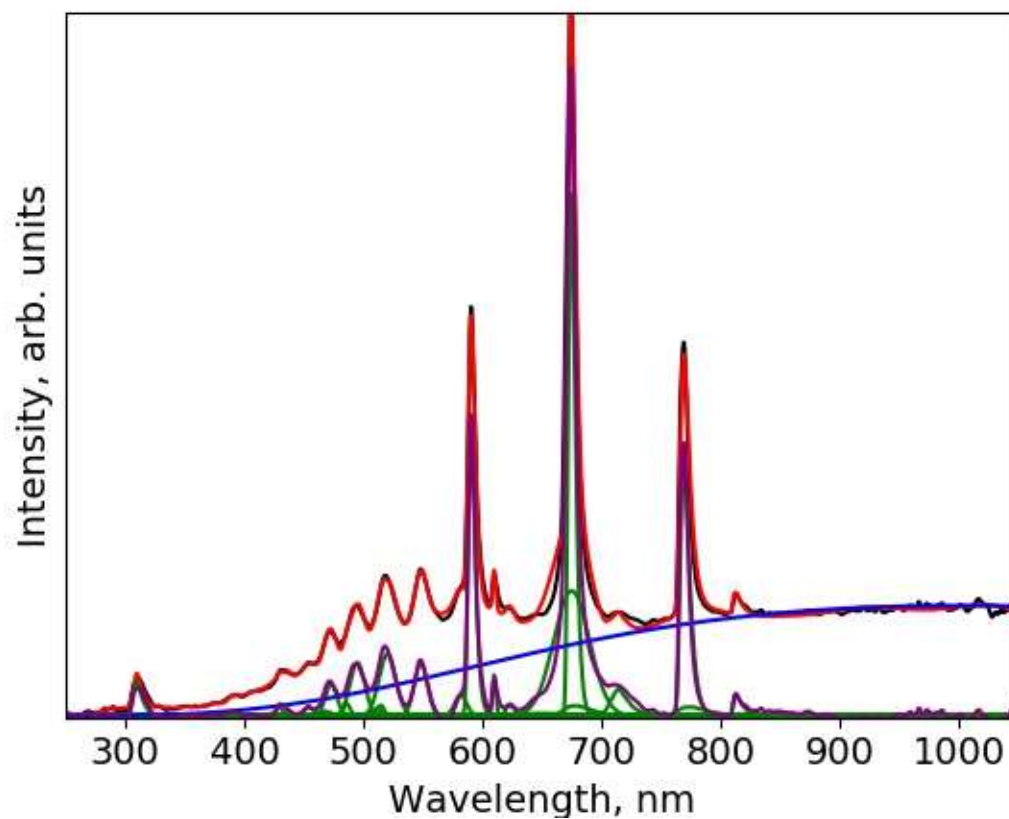


Figure S5. Simulation of representative emission spectrum of JP-10/TiAlB RMNPs droplet combustion with the deconvolution routine described. Black curve is the data, red curve is the simulation, green lines are spectral feature of the individual species. Blue curve is the blackbody radiation obtained by fitting the baseline to a modified Planck's formula.

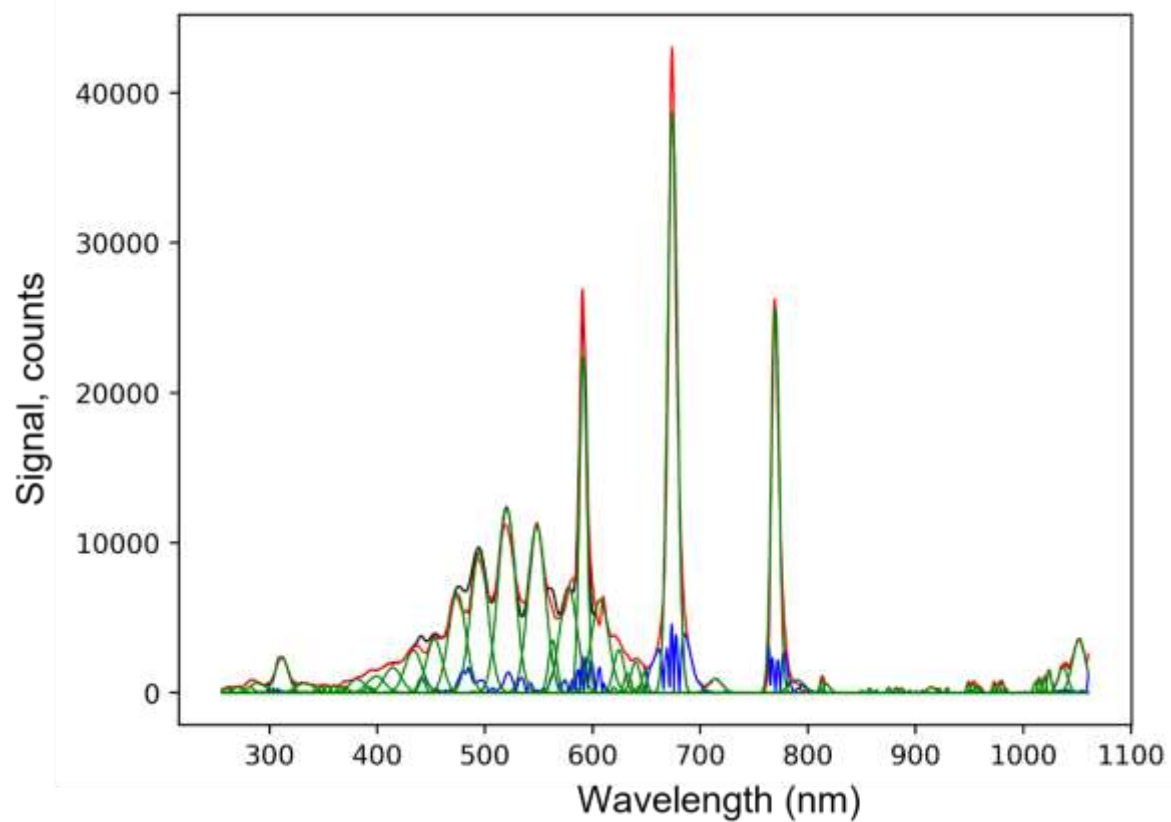
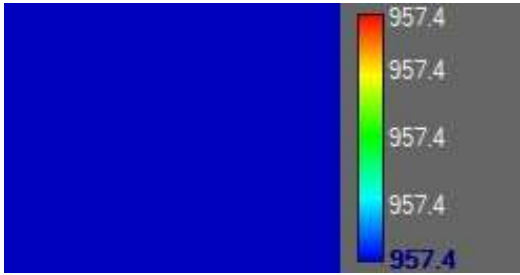
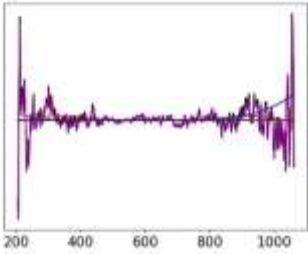
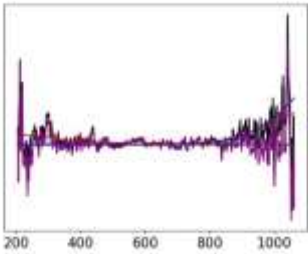
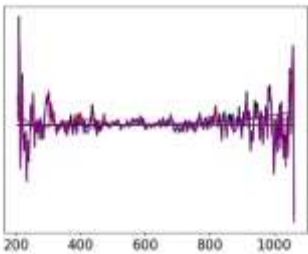
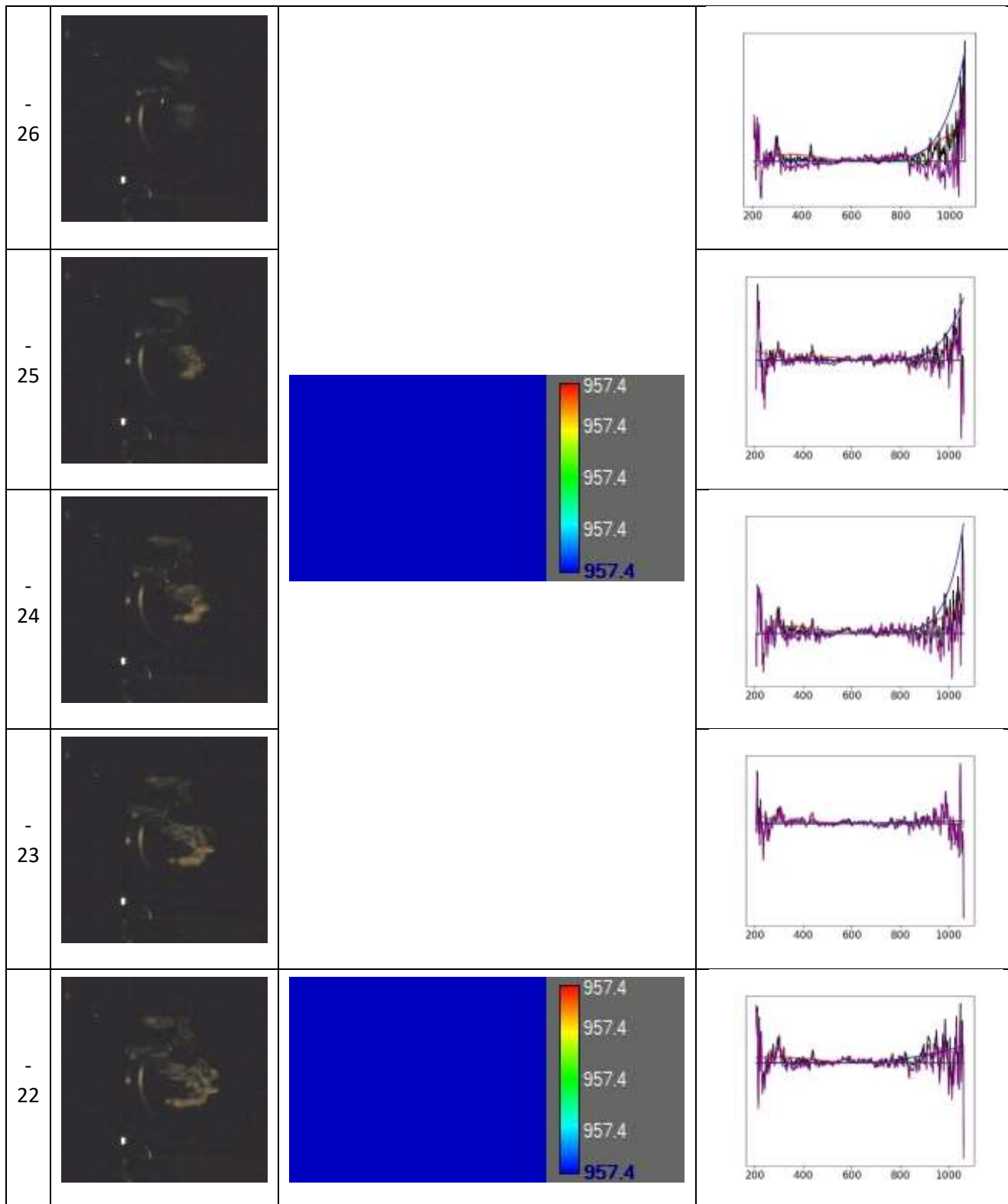
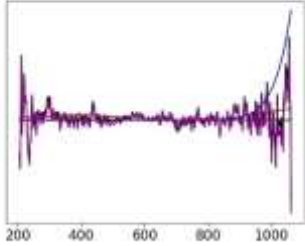
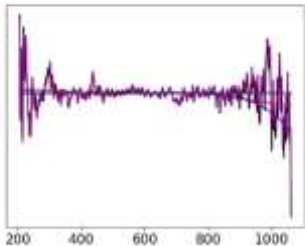
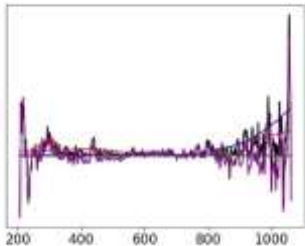
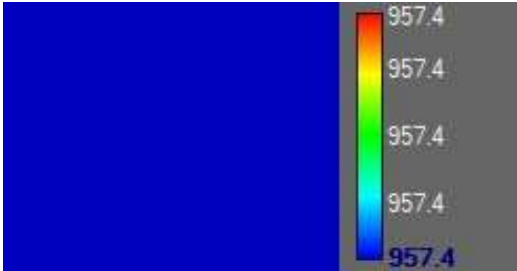
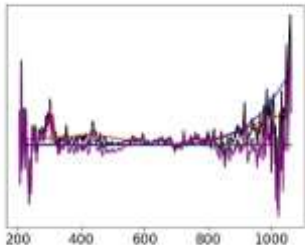
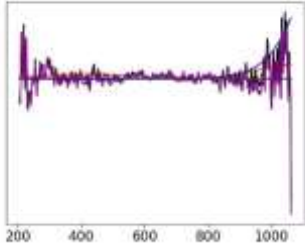


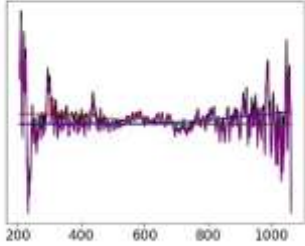
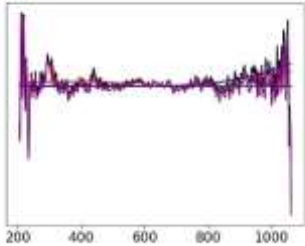
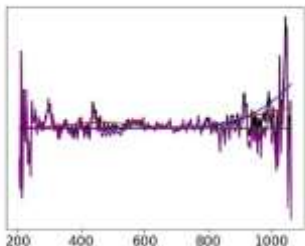
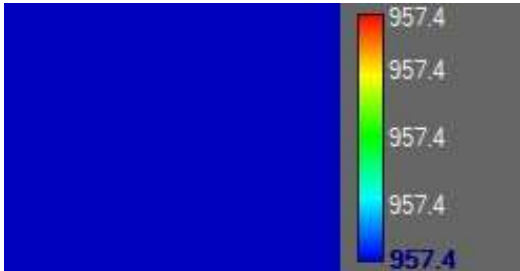
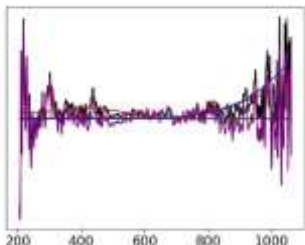
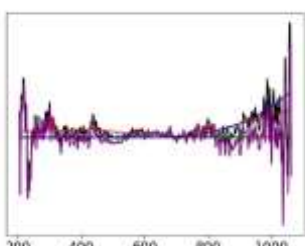
Figure S6. Example of the automated Gaussian deconvolution of a representative JP-10/TiAlB RMNPs emission spectrum. Red curve is the data, black curve is the simulation, green lines are the individual Gaussian peaks, blue curve is the residual.

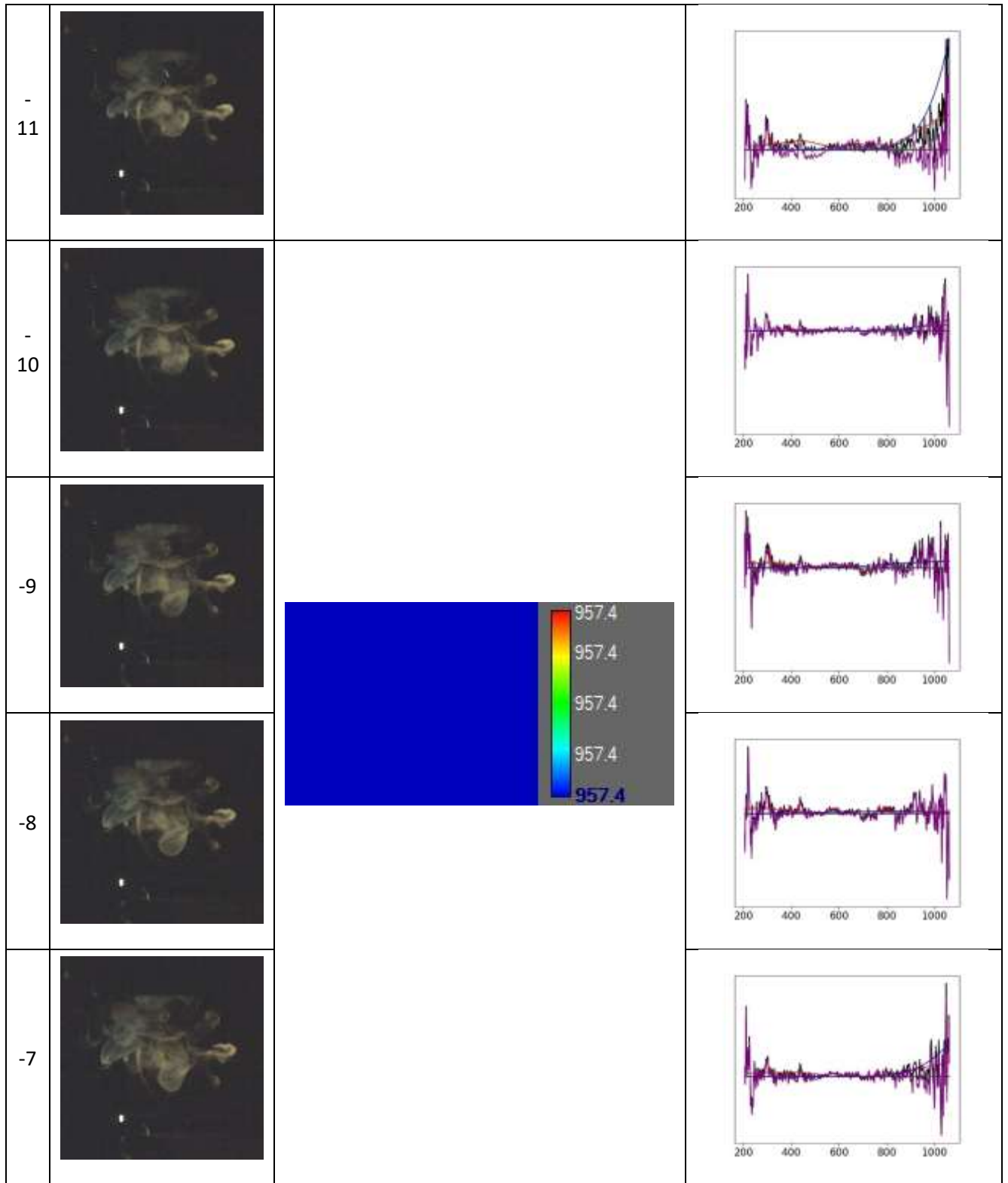
Table S1. Synchronized emission spectra, optical and IR images of combustion for the JP-10/AINPs system. Temperatures are given in units of °C.

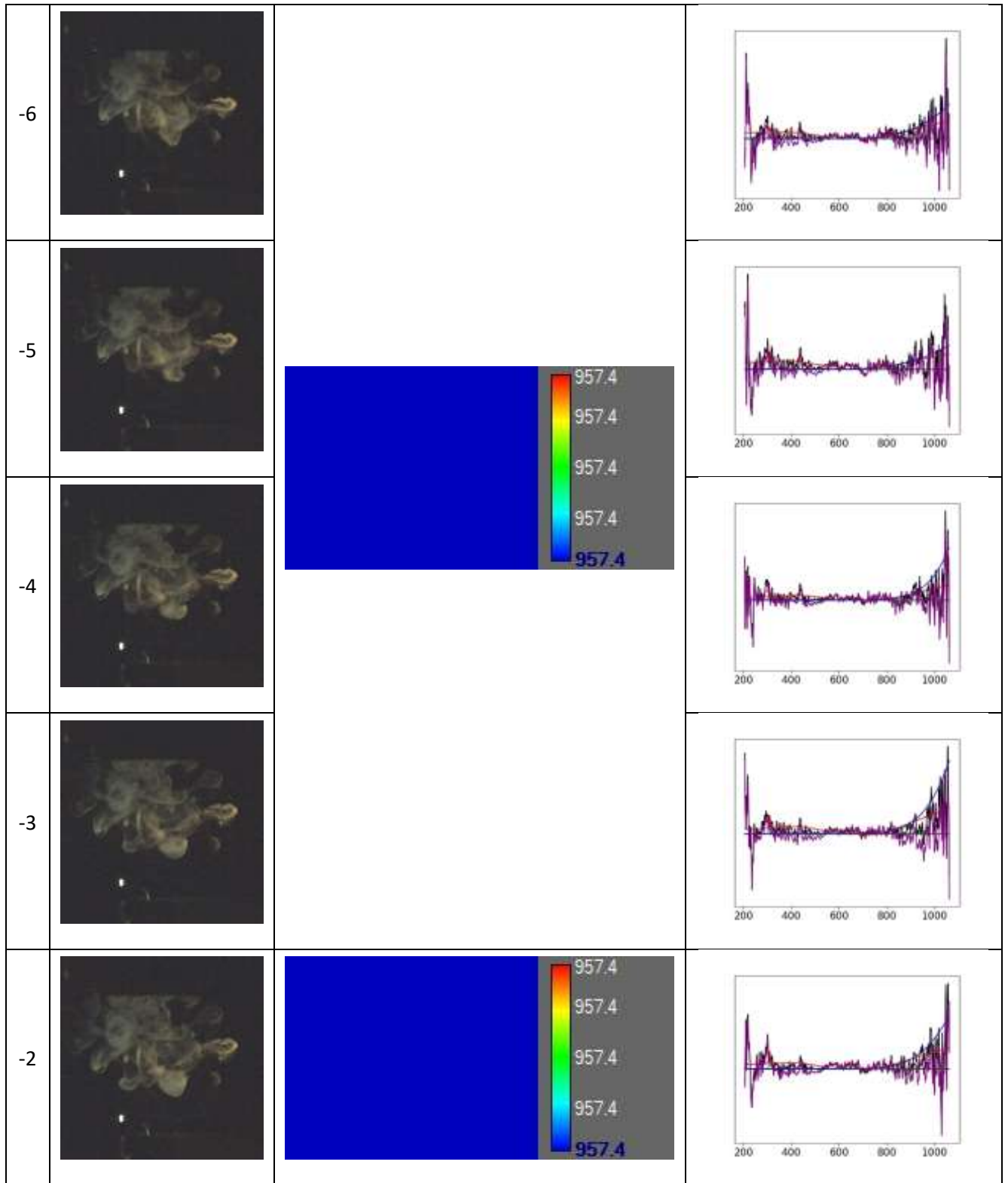
| Time, ms | Video | IR camera | Emission spectrum | |
|----------|---|---|-------------------|---|
| -30 |  |  | | |
| -29 |  | | |  |
| -28 |  | | |  |
| -27 |  | | |  |

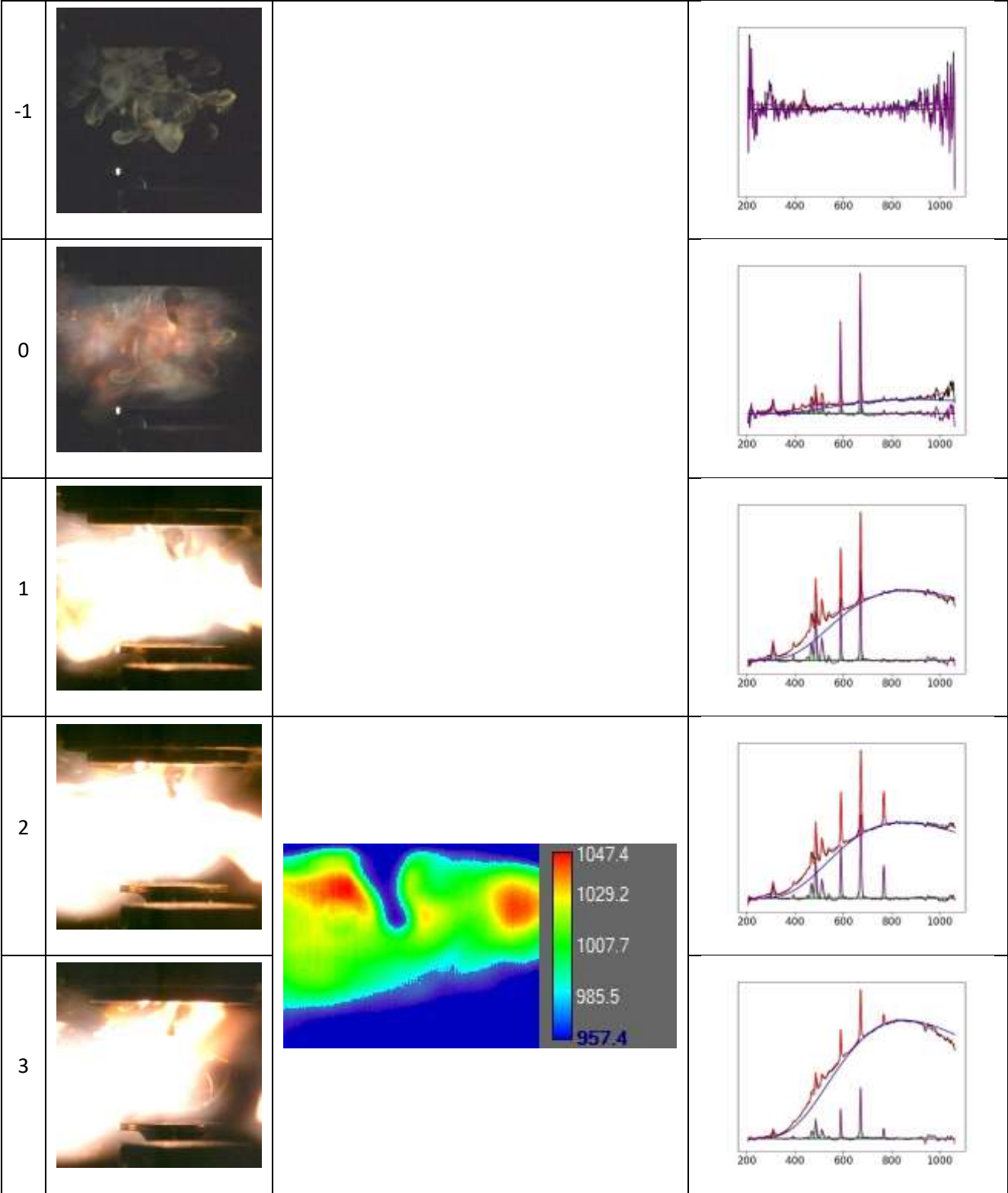


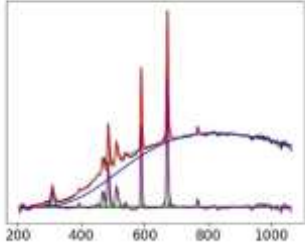
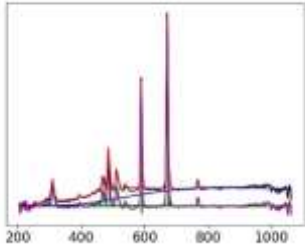
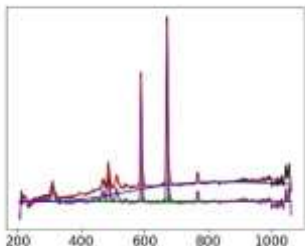
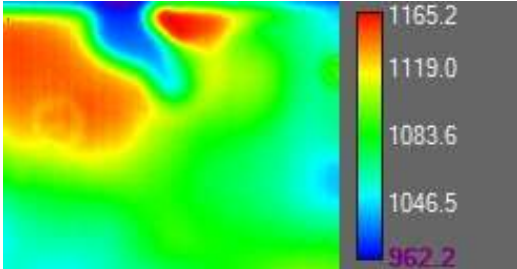
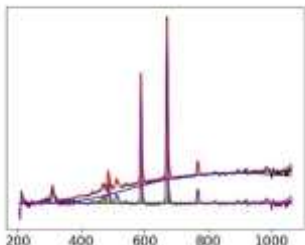
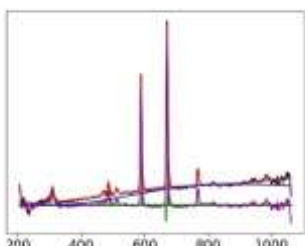
| | | | |
|---------|---|--|---|
| - 21 |  | |  |
| - 20 |  | |  |
| - 19 |  | |  |
| - 18 |  |  |  |
| - 17 |  | |  |

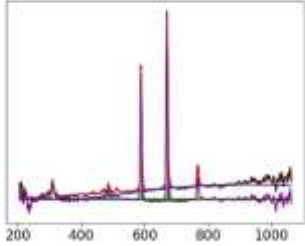
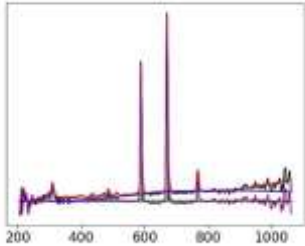
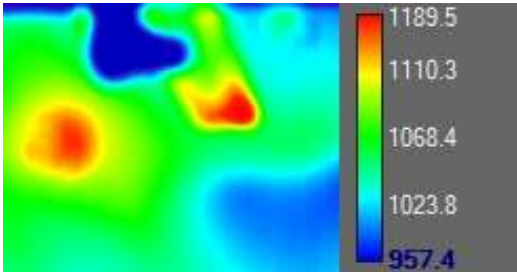
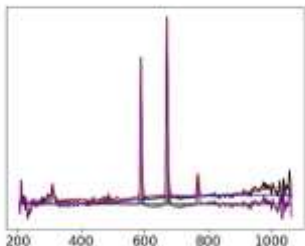
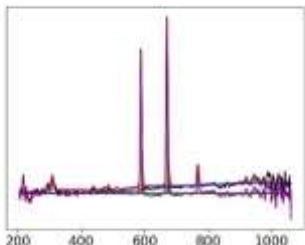
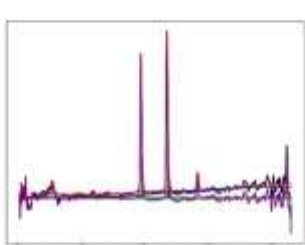
| | | | |
|---------|---|--|---|
| - 16 |  | |  |
| - 15 |  | |  |
| - 14 |  | |  |
| - 13 |  |  |  |
| - 12 |  | |  |

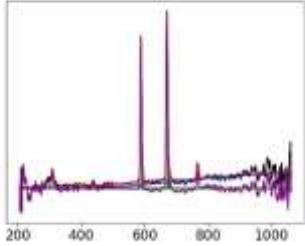
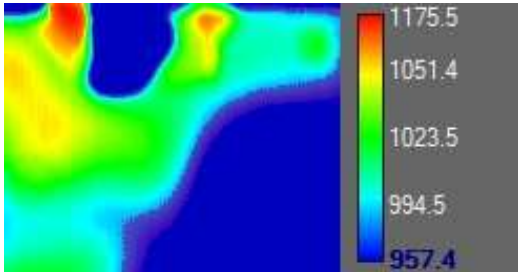
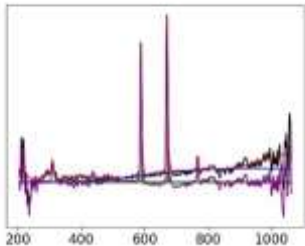
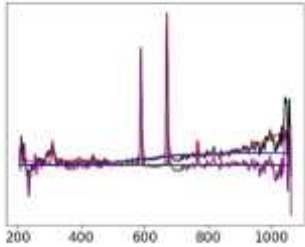
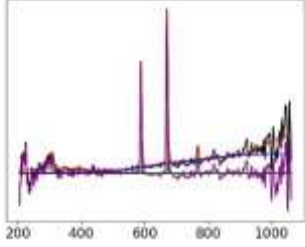
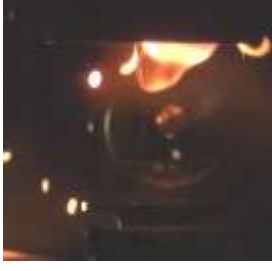
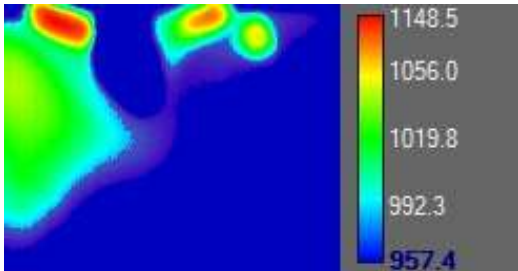
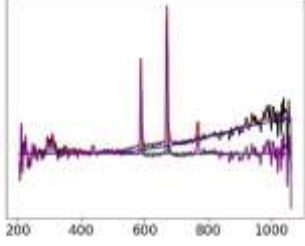


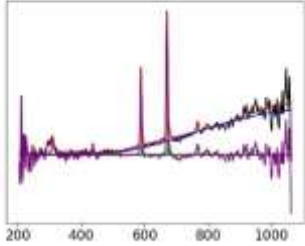
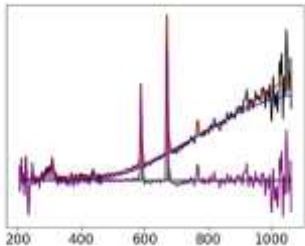
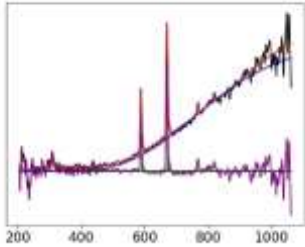
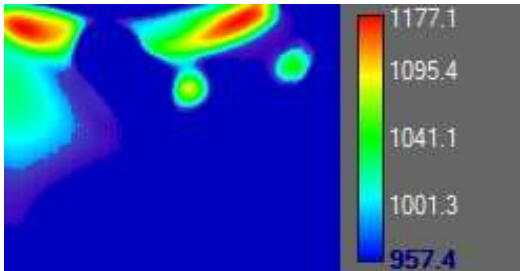
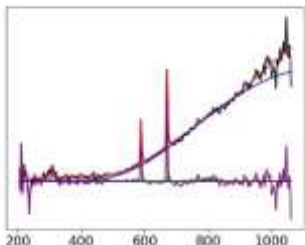
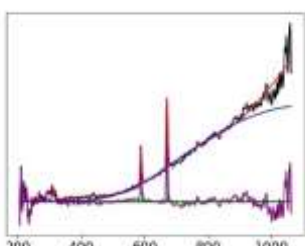


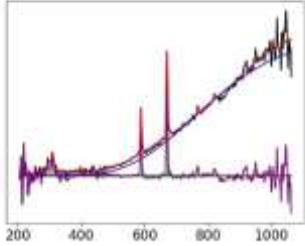
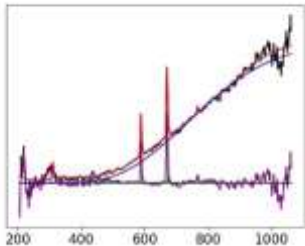
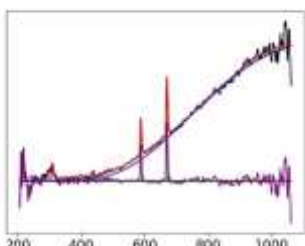
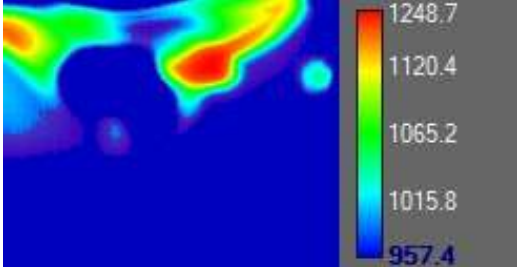
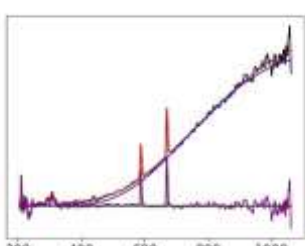
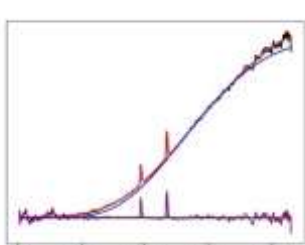


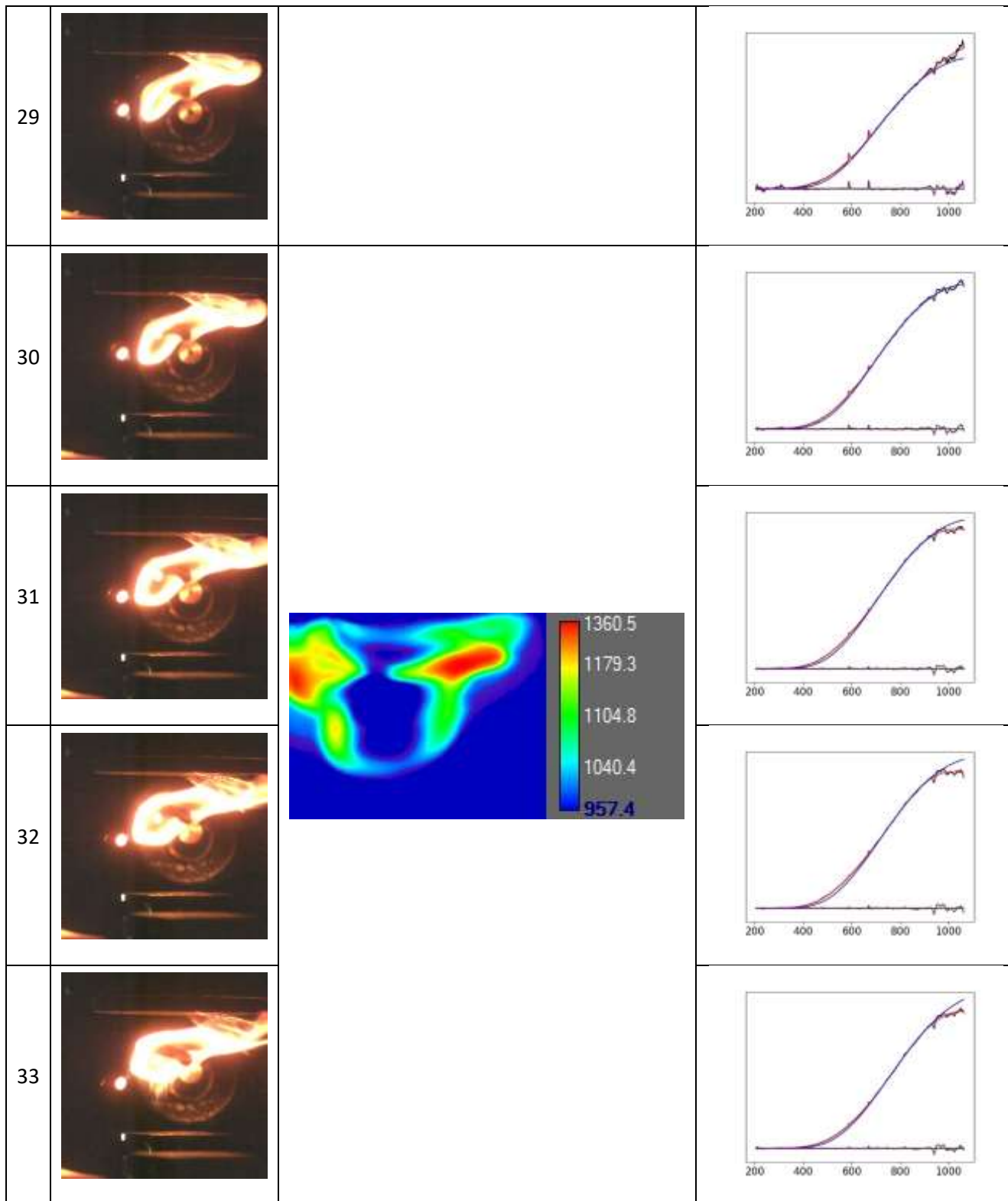
| | | | |
|---|---|--|---|
| 4 |  | |  |
| 5 |  | |  |
| 6 |  | |  |
| 7 |  |  |  |
| 8 |  | |  |

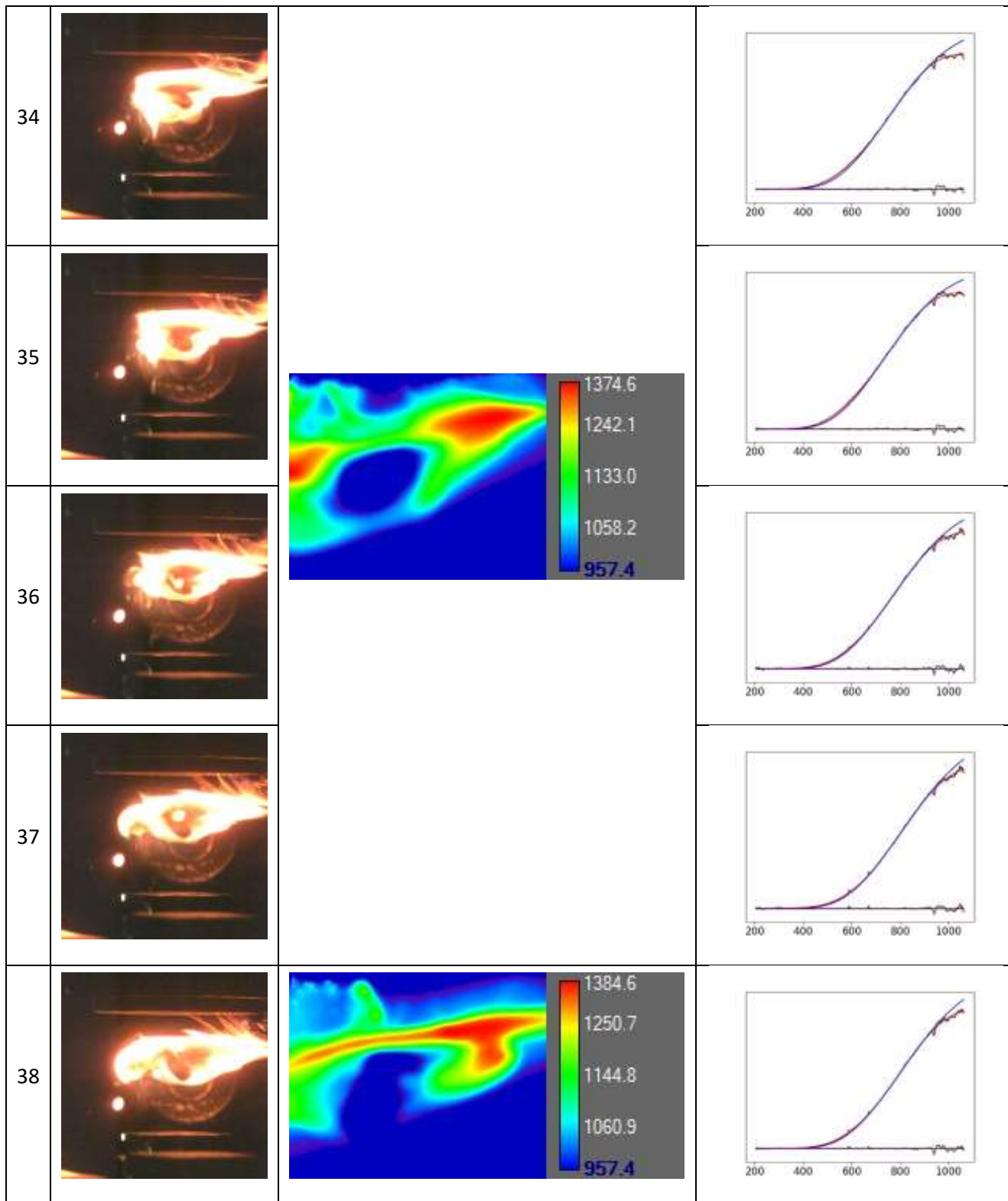
| | | | |
|----|---|---|---|
| 9 |  | |  |
| 10 |  | |  |
| 11 |  |  |  |
| 12 |  | |  |
| 13 |  | |  |

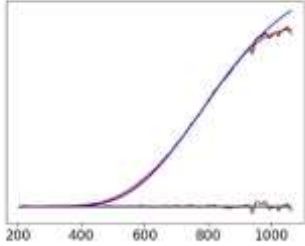
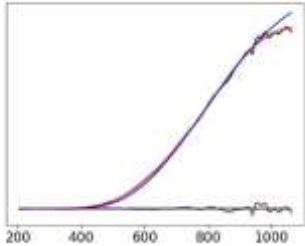
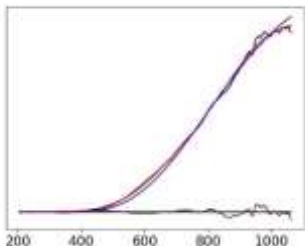
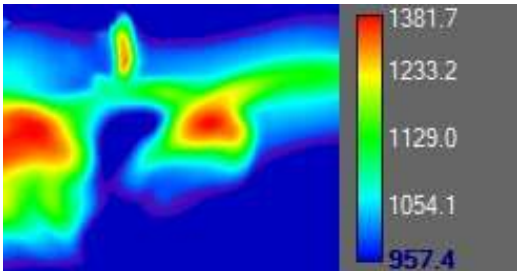
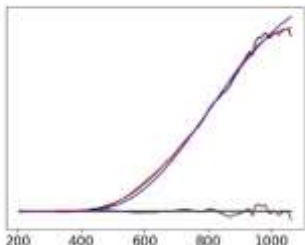
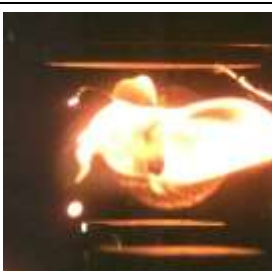
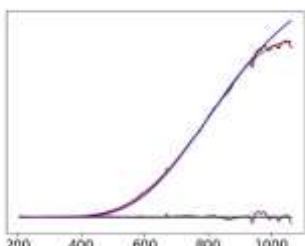
| | | | |
|----|---|--|---|
| 14 |  | |  |
| 15 |  |  |  |
| 16 |  | |  |
| 17 |  | |  |
| 18 |  |  |  |

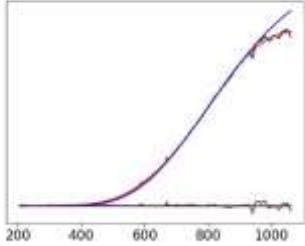
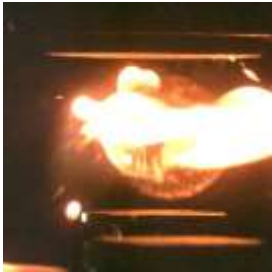
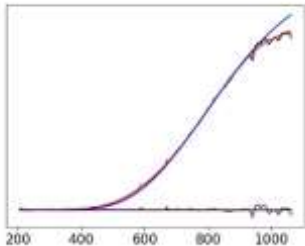
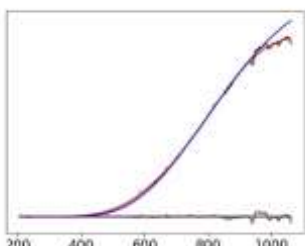
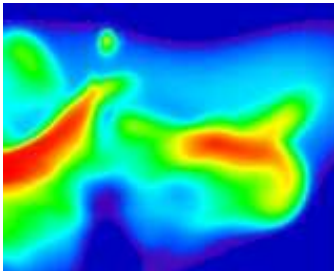
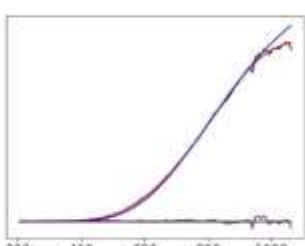
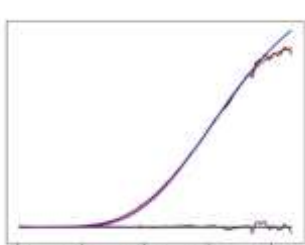
| | | | |
|----|---|--|---|
| 19 |  | |  |
| 20 |  | |  |
| 21 |  | |  |
| 22 |  |  |  |
| 23 |  | |  |

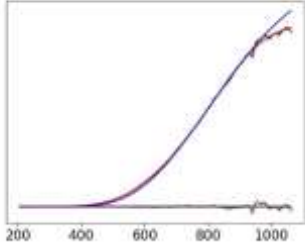
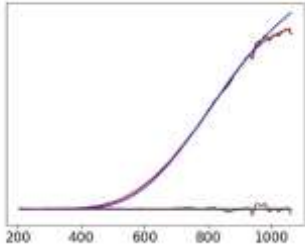
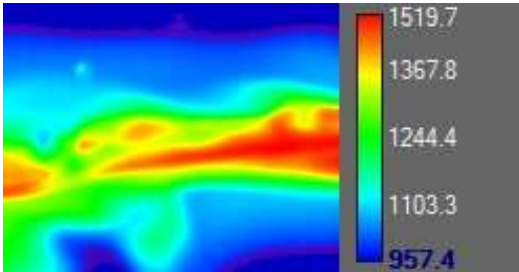
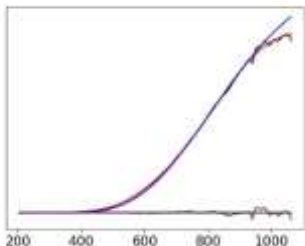
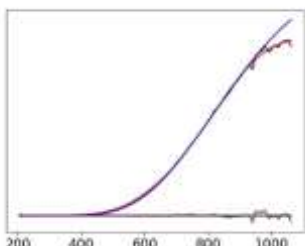
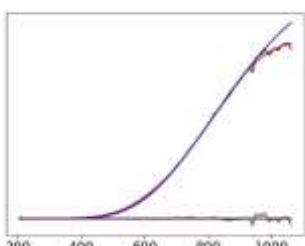
| | | | |
|----|---|--|---|
| 24 |  | |  |
| 25 |  | |  |
| 26 |  | |  |
| 27 |  |  |  |
| 28 |  | |  |

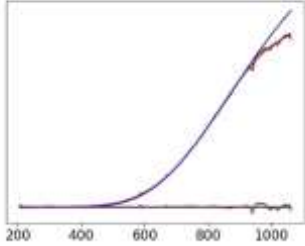
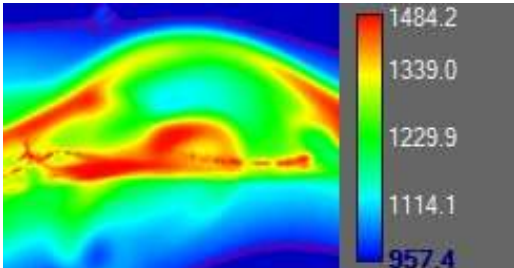
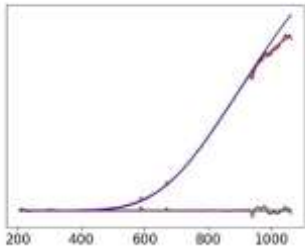
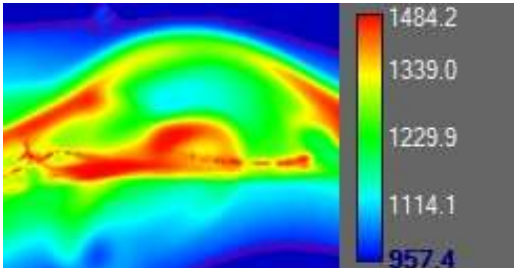
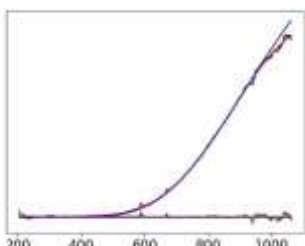
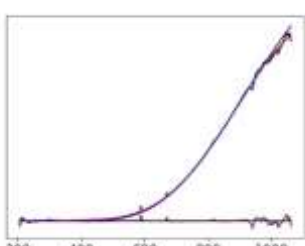
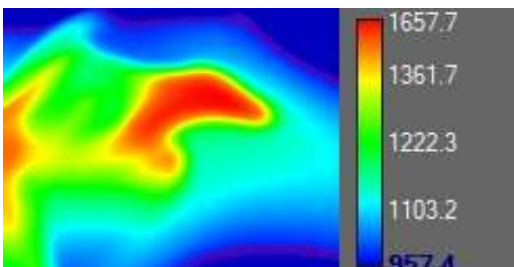
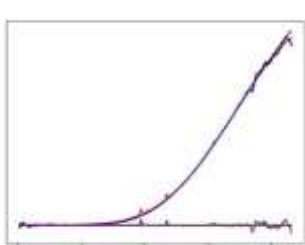


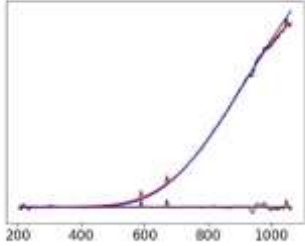
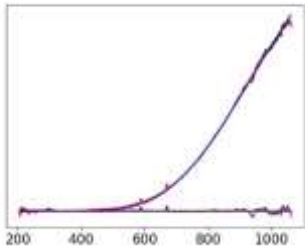
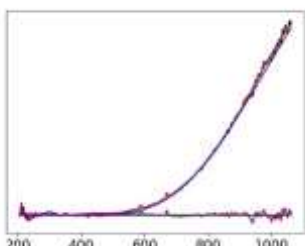
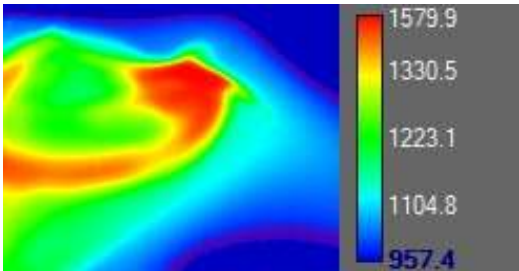
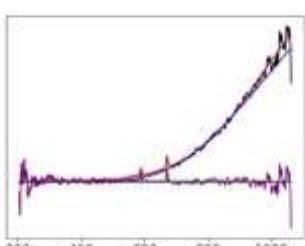
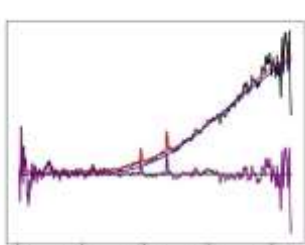


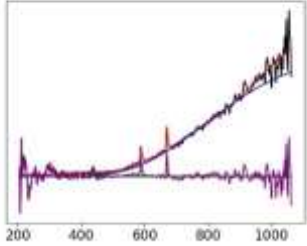
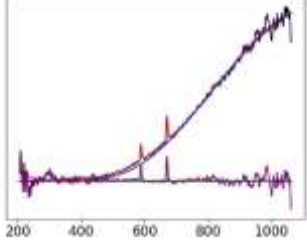
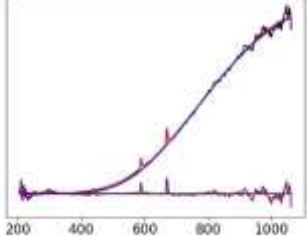
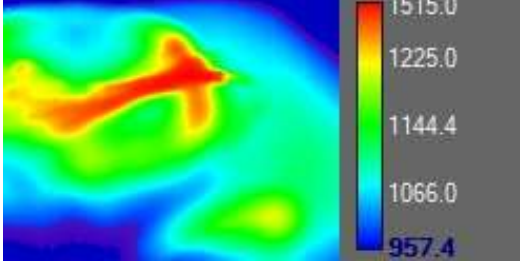
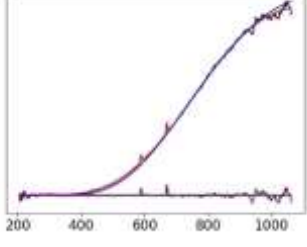
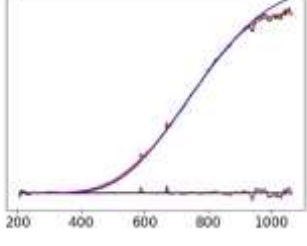
| | | | |
|----|---|--|---|
| 39 |  | |  |
| 40 |  | |  |
| 41 |  | |  |
| 42 |  |  |  |
| 43 |  | |  |

| | | | |
|----|---|--|---|
| 44 |  | |  |
| 45 |  | |  |
| 46 |  | |  |
| 47 |  |  <div data-bbox="906 1134 1073 1402"> <p>1494.0 1272.3 1160.2 1072.1 957.4</p> </div> |  |
| 48 |  | |  |

| | | | |
|----|---|---|---|
| 49 |  | |  |
| 50 |  | |  |
| 51 |  |  |  |
| 52 |  | |  |
| 53 |  | |  |

| | | | |
|----|---|--|---|
| 54 |  | |  |
| 55 |  |  |  |
| 56 |  |  |  |
| 57 |  | |  |
| 58 |  |  |  |

| | | | |
|----|---|--|---|
| 59 |  | |  |
| 60 |  | |  |
| 61 |  | |  |
| 62 |  |  |  |
| 63 |  | |  |

| | | | |
|----|---|---|---|
| 64 |  | |  |
| 65 |  | |  |
| 66 |  | |  |
| 67 |  |  <p>1515.0 1225.0 1144.4 1066.0 957.4</p> |  |
| 68 |  | |  |

69

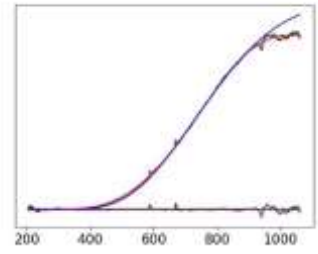
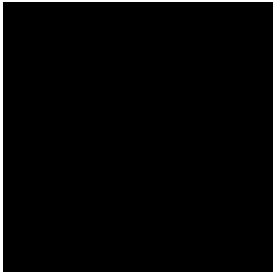
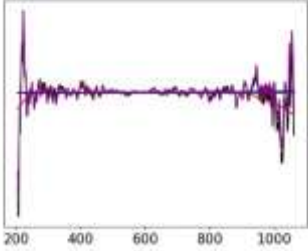
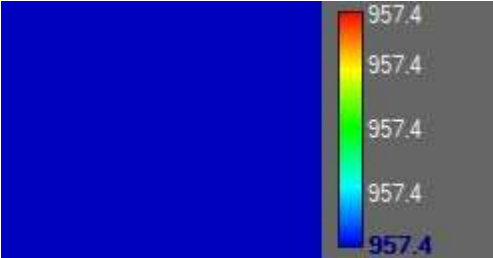
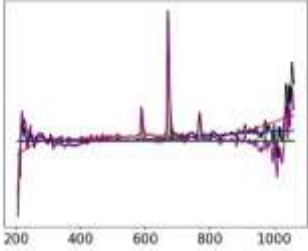
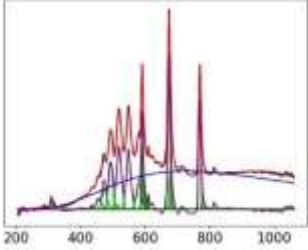
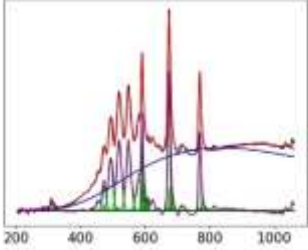
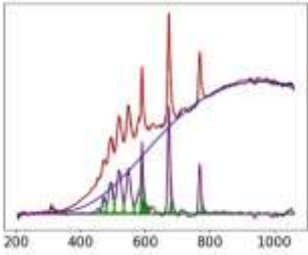
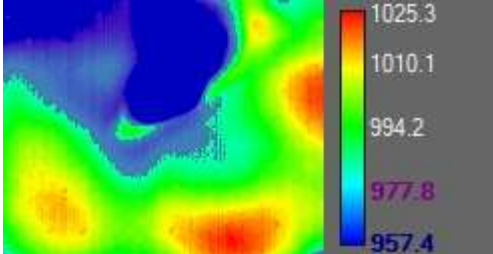
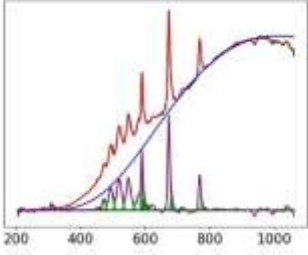
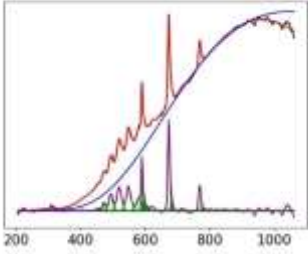
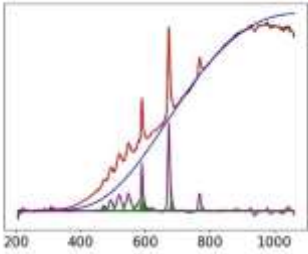
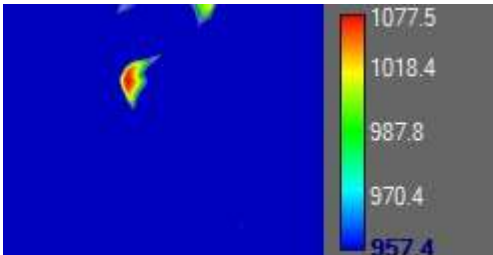
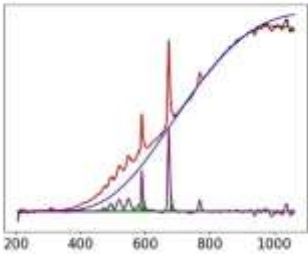
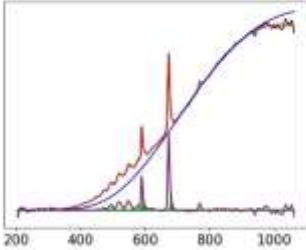
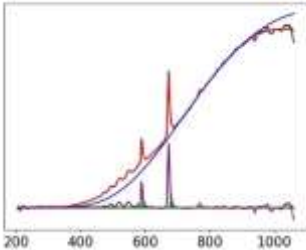
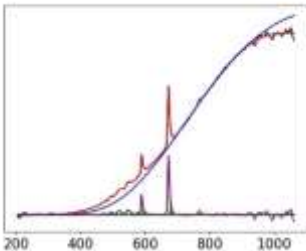
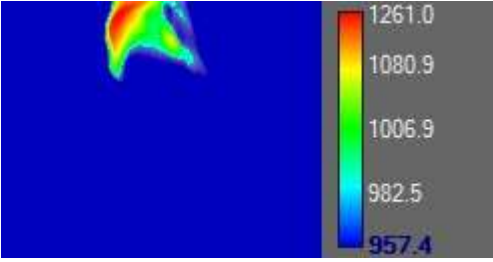
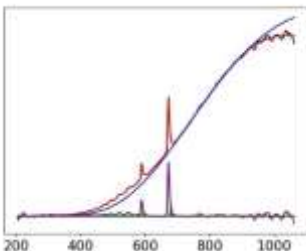
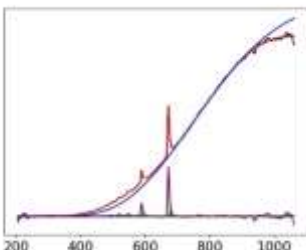
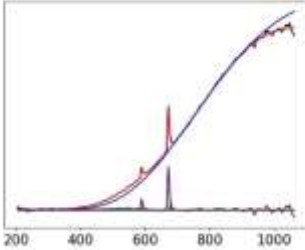
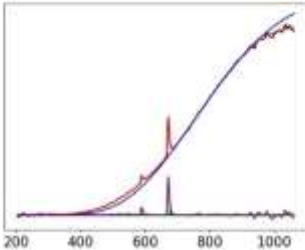
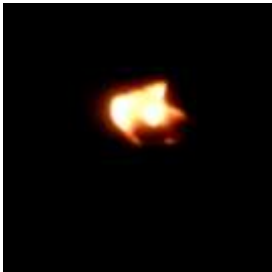
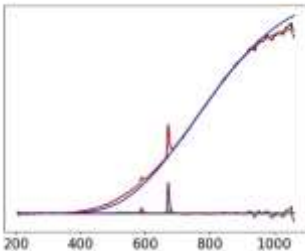
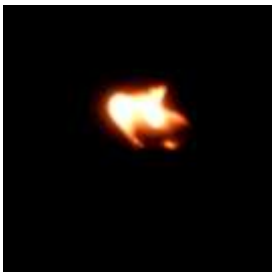
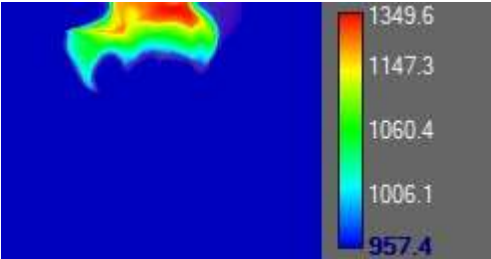
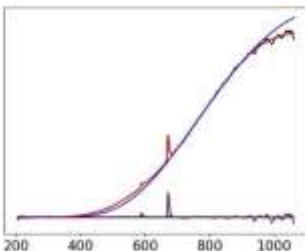
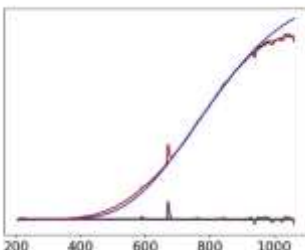


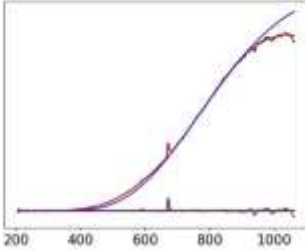
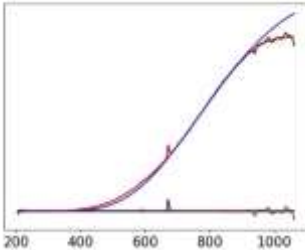
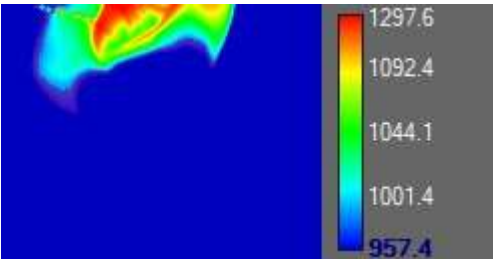
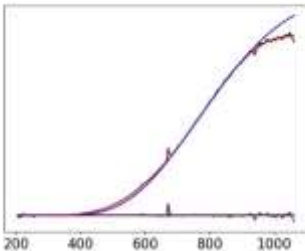
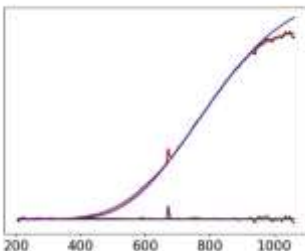
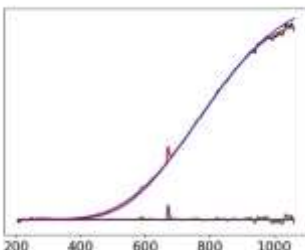
Table S2. Synchronized emission spectra, optical and IR images of combustion for the JP-10/Ti-Al-B-RMNPs system. Temperatures are given in units of °C.

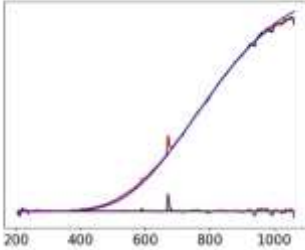
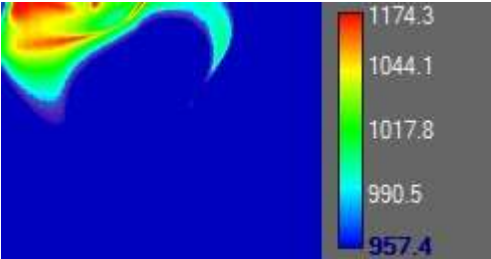
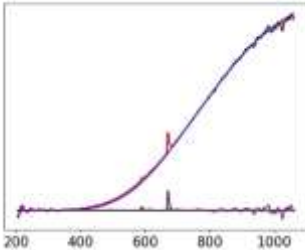
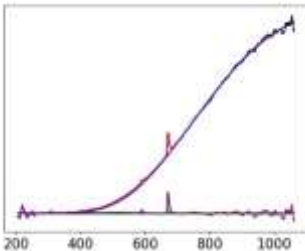
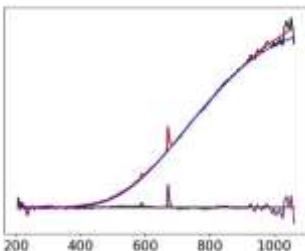
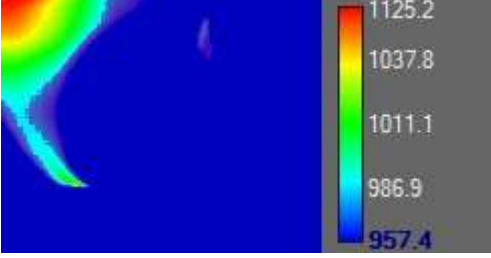
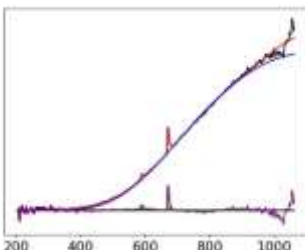
| Time, ms | Video | IR camera | Emission spectrum |
|----------|---|---|---|
| -1 |  | |  |
| 0 |  |  |  |
| 1 |  | |  |
| 2 |  | |  |

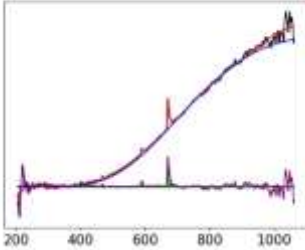
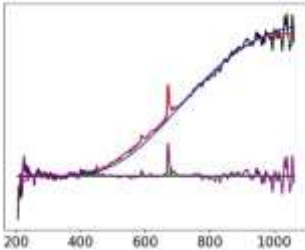
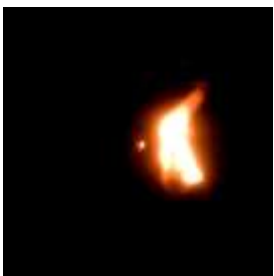
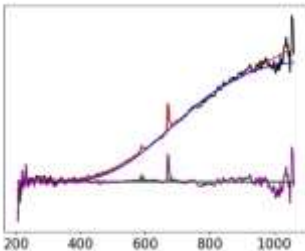
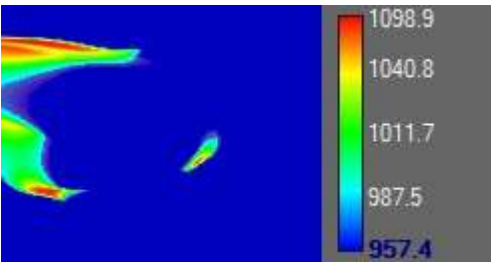
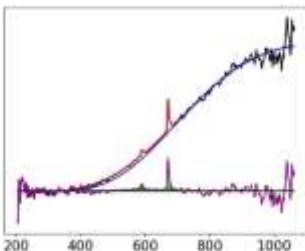
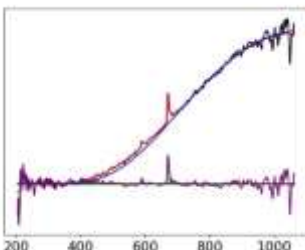
| | | | |
|---|---|--|---|
| 3 |  | |  |
| 4 |  |  |  |
| 5 |  | |  |
| 6 |  | |  |
| 7 |  |  |  |

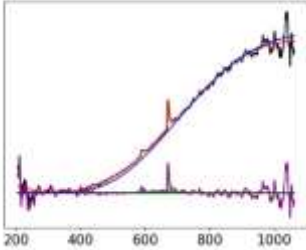
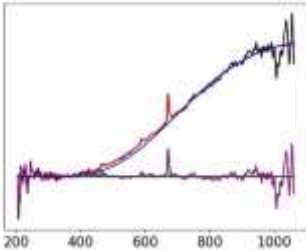
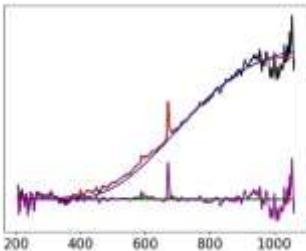
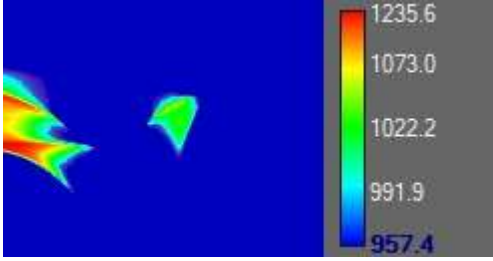
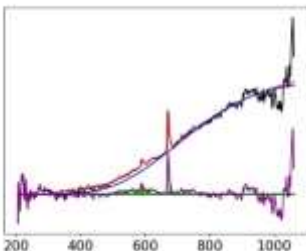
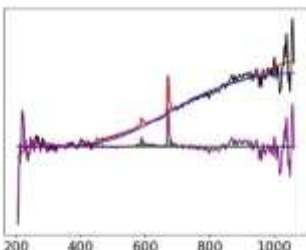
| | | | |
|----|---|--|---|
| 8 |  | |  |
| 9 |  | |  |
| 10 |  | |  |
| 11 |  |  |  |
| 12 |  | |  |

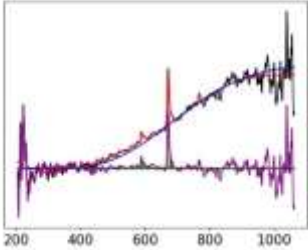
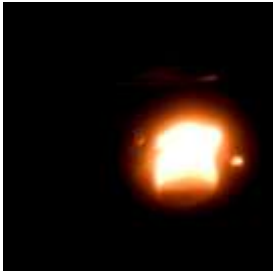
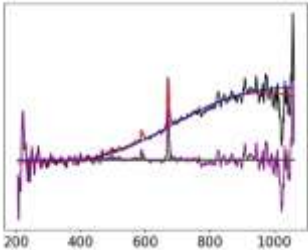
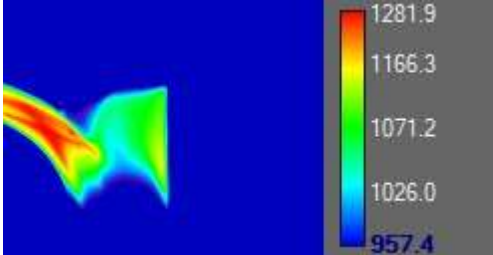
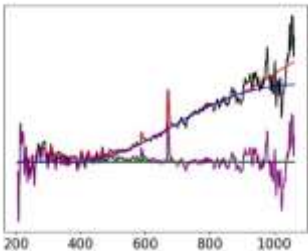
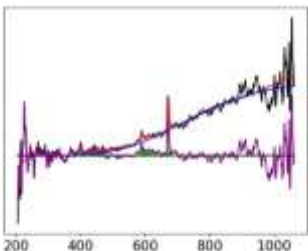
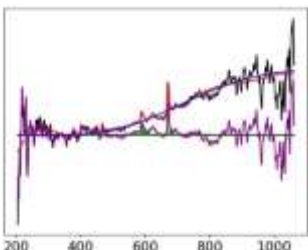
| | | | |
|----|---|--|---|
| 13 |  | |  |
| 14 |  | |  |
| 15 |  | |  |
| 16 |  |  |  |
| 17 |  | |  |

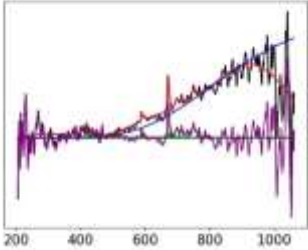
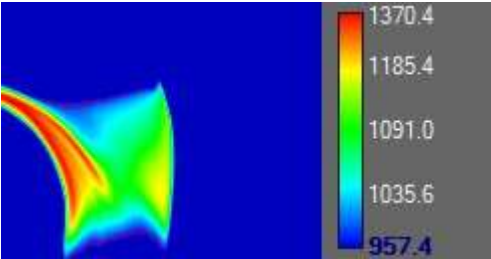
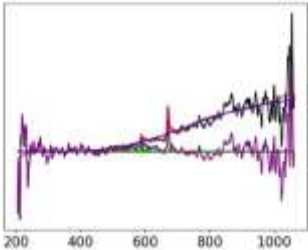
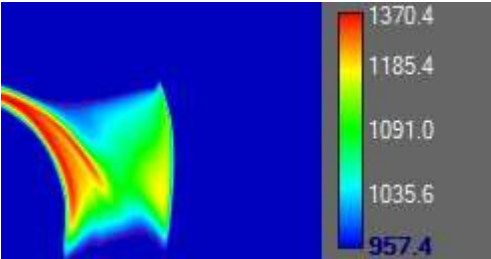
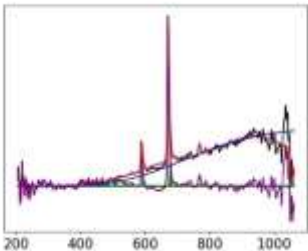
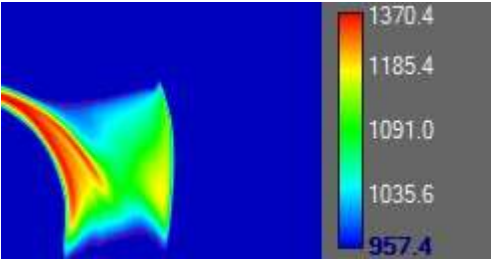
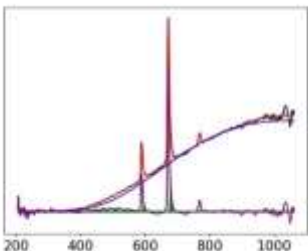
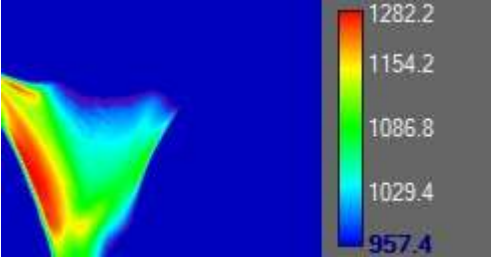
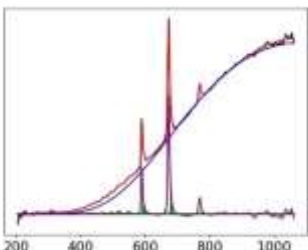
| | | | |
|----|---|---|---|
| 18 |  | |  |
| 19 |  | |  |
| 20 |  |  |  |
| 21 |  | |  |
| 22 |  | |  |

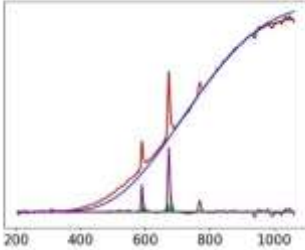
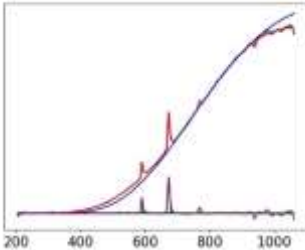
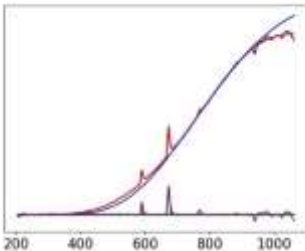
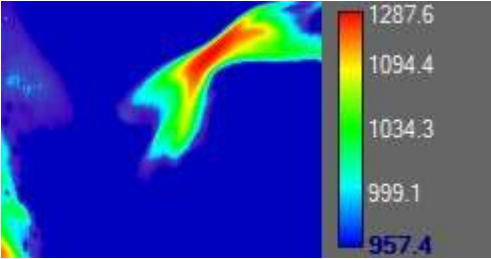
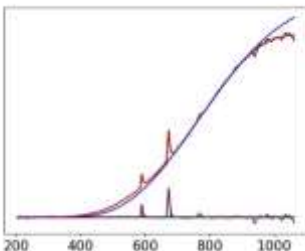
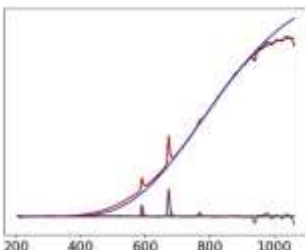
| | | | |
|----|---|--|---|
| 23 |  | |  |
| 24 |  |  |  |
| 25 |  | |  |
| 26 |  | |  |
| 27 |  |  |  |

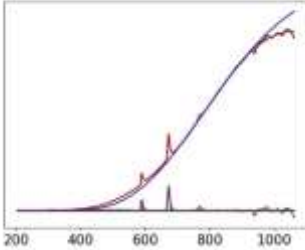
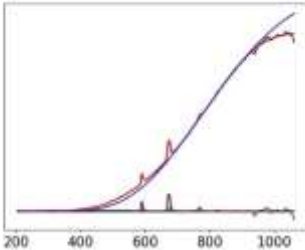
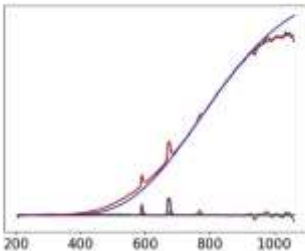
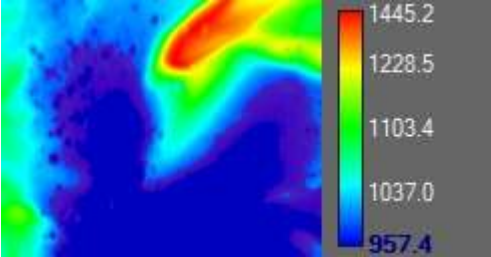
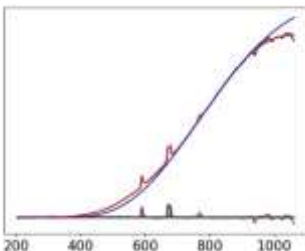
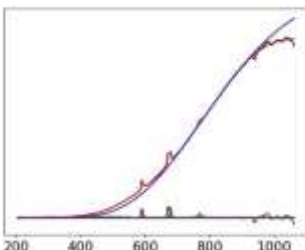
| | | | |
|----|---|--|---|
| 28 |  | |  |
| 29 |  | |  |
| 30 |  | |  |
| 31 |  |  |  |
| 32 |  | |  |

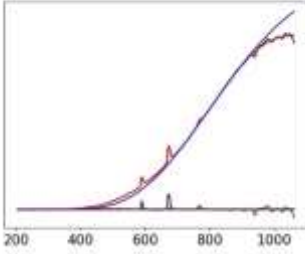
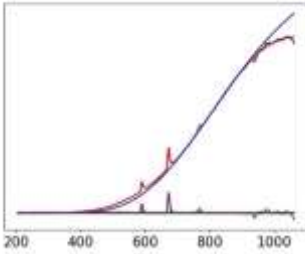
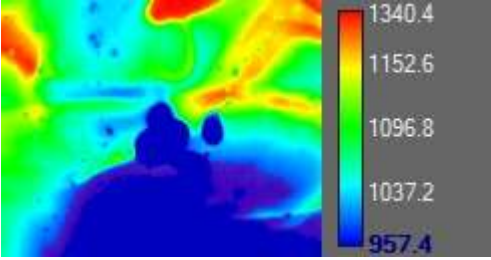
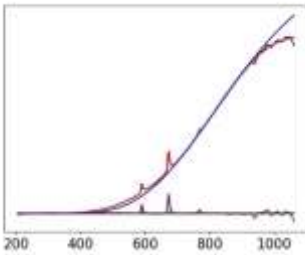
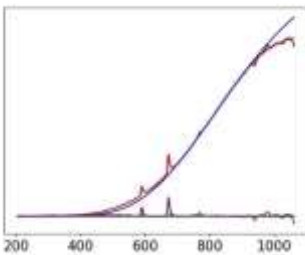
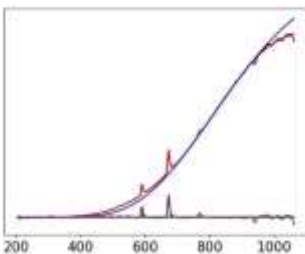
| | | | |
|----|---|--|---|
| 33 |  | |  |
| 34 |  | |  |
| 35 |  | |  |
| 36 |  |  |  |
| 37 |  | |  |

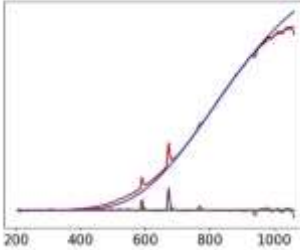
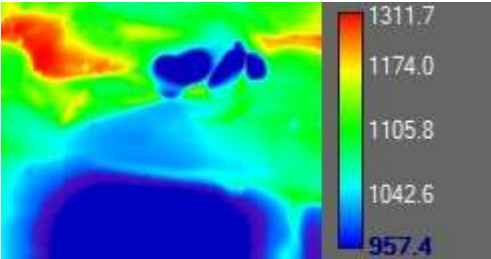
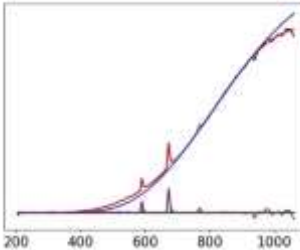
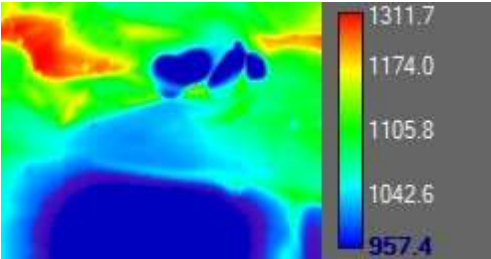
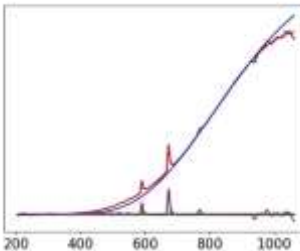
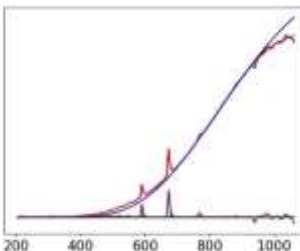
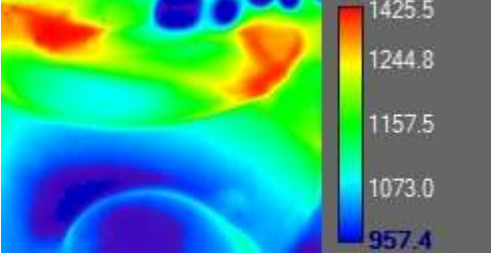
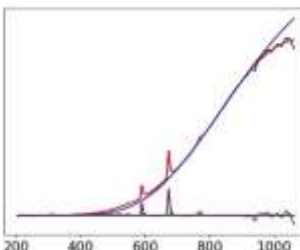
| | | | |
|----|---|--|---|
| 38 |  | |  |
| 39 |  | |  |
| 40 |  |  |  |
| 41 |  | |  |
| 42 |  | |  |

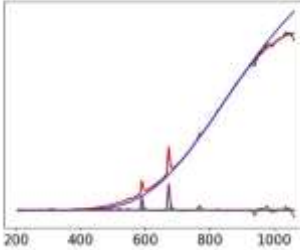
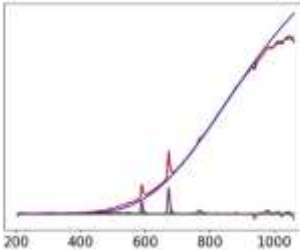
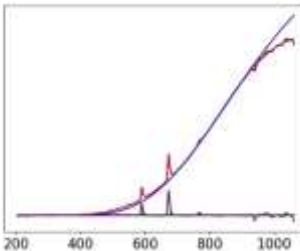
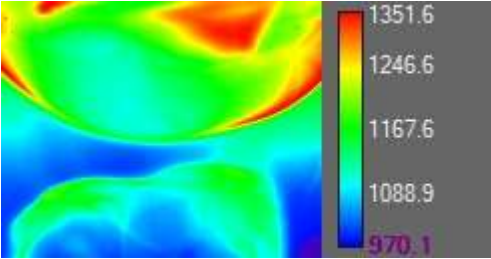
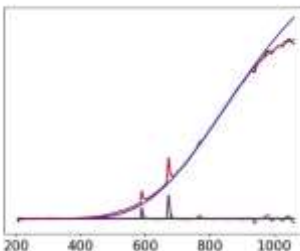
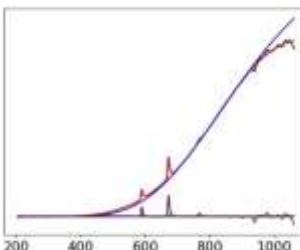
| | | | |
|----|---|--|---|
| 43 |  | |  |
| 44 |  |  |  |
| 45 |  |  |  |
| 46 |  |  |  |
| 47 |  |  |  |

| | | | |
|----|---|--|---|
| 48 |  | |  |
| 49 |  | |  |
| 50 |  | |  |
| 51 |  |  |  |
| 52 |  | |  |

| | | | |
|----|---|--|---|
| 53 |  | |  |
| 54 |  | |  |
| 55 |  | |  |
| 56 |  |  |  |
| 57 |  | |  |

| | | | |
|----|---|--|---|
| 58 |  | |  |
| 59 |  | |  |
| 60 |  |  |  |
| 61 |  | |  |
| 62 |  | |  |

| | | | |
|----|---|--|---|
| 63 |  | |  |
| 64 |  |  |  |
| 65 |  |  |  |
| 66 |  | |  |
| 67 |  |  |  |

| | | | |
|----|---|--|---|
| 68 |  | |  |
| 69 |  | |  |
| 70 |  | |  |
| 71 |  |  |  |
| 72 |  | |  |

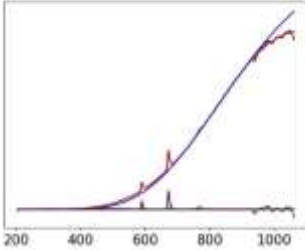
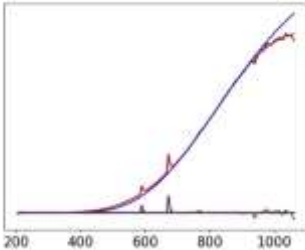
| | | | |
|----|---|--|---|
| 73 |  | |  |
| 74 |  | |  |

Table S3. Deconvolution and peak assignment for the flame emission spectrum of JP10 – AINPs taken at 0 ms (Fig. 2A).

| Peak /band | Peak wavelength / band center (nm) ^{a)} | Carrier | Reference wavelength (nm) | Transition | Branch; spin-orbit components; vibrational quantum numbers: (v', v'') or (v ₁ ', v ₂ ', v ₃ ') - (v ₁ '', v ₂ '', v ₃ '') |
|------------|--|-----------------------|--|--|---|
| a | 294.8 | Na | 285.3 ^a | 5p ² P ^o - 3s ² S | 3/2 - 1/2; 1/2 - 1/2 |
| b | 308.8 | OH | 309.9 ^b | A ² Σ ⁺ - X ² Π | (0-0), (1-1) |
| c | 394.1 | Al | 394.4, 396.1 ^a | 4s ² S - 3p ² P ^o | 1/2 - 1/2; 1/2 - 3/2 |
| d | 429.2 | CH | 429.6 ^b | A ² Σ ⁺ - X ² Π | (0-0), (1-1), (2-2) |
| e | 438.0 | C ₂ | 435.4 ^b | d ³ Π _g - a ³ Π _u | (2-0), (3-1) |
| f | 453.3 | AlO | 452.6 ^b | B ² Σ ⁺ - X ² Σ ⁺ | (2-0) |
| g | 468.8 | C ₂ AlO | ^b 467.6 ^b | d ³ Π _g - a ³ Π _u B ² Σ ⁺ - X ² Σ ⁺ | (1-0), (2-1), (3-2) (1-0), (2-1) |
| h | 486.3 | AlO | 486.0 ^b | B ² Σ ⁺ - X ² Σ ⁺ | (0-0), (1-1) |
| i | 512.3 | C ₂ AlO | 515.0 ^b 511.2 ^b | d ³ Π _g - a ³ Π _u B ² Σ ⁺ - X ² Σ ⁺ | (0-0), (1-1) (0-1), (1-2) |
| j | 543.8 | C ₂ AlO | 549.5 ^b 540.2 ^b | d ³ Π _g - a ³ Π _u B ² Σ ⁺ - X ² Σ ⁺ | (3-4) (2-3) |
| k | 559.9 | C ₂ | 559.8 ^b | d ³ Π _g - a ³ Π _u | (0-1), (1-2), (2-3) |
| l | 588.0 | Na | 589.0 ^a | 3p ² P ^o - 3s ² S | 3/2 - 1/2; 1/2 - 1/2 |
| m | 590.4 | Na | 589.6 ^a | 3p ² P ^o - 3s ² S | 3/2 - 1/2; 1/2 - 1/2 |
| n | 669.5 | Li | 670.8 ^a | 2p ² P ^o - 2s ² S | 3/2 - 1/2; 1/2 - 1/2 |
| o | 671.3 | Li | 670.8 ^a | 2p ² P ^o - 2s ² S | 3/2 - 1/2; 1/2 - 1/2 |
| p | 673.6 | Li | 670.8 ^a | 2p ² P ^o - 2s ² S | 3/2 - 1/2; 1/2 - 1/2 |
| q | 766.6 | K | 766.5 ^a | 4p ² P ^o - 4s ² S | 3/2 - 1/2; 1/2 - 1/2 |

Table S4. Deconvolution and peak assignment for the flame emission spectrum of JP10 – AINPs taken at 4 ms (Fig. 2B).

| Peak /band | Peak wavelength / band center (nm) ^a | Carrier | Reference wavelength (nm) | Transition | Branch; spin-orbit components; vibrational quantum numbers: (v', v'') or (v ₁ , v ₂ , v ₃ ') - (v ₁ '', v ₂ '', v ₃ '') |
|------------|---|----------------|---------------------------|---|---|
| a | 290.2 | Na | 285.3 ^a | 5p ² P ^o - 3s ² S | 3/2 - 1/2; 1/2 - 1/2 |
| b | 308.7 | OH | 309.9 ^b | A ² Σ ⁺ - X ² Π | (0-0) |
| c | 318.0 | OH | 314.5 ^b | A ² Σ ⁺ - X ² Π | (1-1) |
| d | 393.7 | Al | 394.4, 396.1 ^a | 4s ² S - 3p ² P ^o | 1/2 - 1/2; 1/2 - 3/2 |
| e | 437.4 | C ₂ | 435.4 ^b | d ³ Π _g - a ³ Π _u | (2-0), (3-1) |
| f | 452.2 | AlO | 452.6 ^b | B ² Σ ⁺ - X ² Σ ⁺ | (2-0) |
| g | 469.7 | AlO | 468.1 ^b | B ² Σ ⁺ - X ² Σ ⁺ | (1-0), (2-1) |
| h | 484.9 | AlO | 485.5 ^b | B ² Σ ⁺ - X ² Σ ⁺ | (0-0) |
| i | 488.2 | AlO | 487.8 ^b | B ² Σ ⁺ - X ² Σ ⁺ | (1-1) |
| j | 510.5 | AlO | 509.2 ^b | B ² Σ ⁺ - X ² Σ ⁺ | (0-1) |
| k | 516.2 | C ₂ | 515.0 ^b | d ³ Π _g - a ³ Π _u | (0-0), (1-1) |
| l | 541.2 | AlO | 540.2 ^b | B ² Σ ⁺ - X ² Σ ⁺ | (2-3) |
| m | 590.3 | Na | 589.0 ^a | 3p ² P ^o - 3s ² S | 3/2 - 1/2; 1/2 - 1/2 |
| n | 591.7 | Na | 589.0 ^a | 3p ² P ^o - 3s ² S | 3/2 - 1/2; 1/2 - 1/2 |
| o | 610.6 | Li | 610.4 ^a | 3d ² D - 2p ² P ^o | 5/2 - 3/2; 3/2 - 3/2; 3/2 - 1/2 |
| p | 663.5 | Li | 670.8 ^a | 2p ² P ^o - 2s ² S | 3/2 - 1/2; 1/2 - 1/2 |
| q | 672.6 | Li | 670.8 ^a | 2p ² P ^o - 2s ² S | 3/2 - 1/2; 1/2 - 1/2 |
| r | 675.8 | Li | 670.8 ^a | 2p ² P ^o - 2s ² S | 3/2 - 1/2; 1/2 - 1/2 |
| s | 776.4 | K | 766.5 ^a | 4p ² P ^o - 4s ² S | 3/2 - 1/2; 1/2 - 1/2 |
| t | 772.5 | K | 766.5 ^a | 4p ² P ^o - 4s ² S | 3/2 - 1/2; 1/2 - 1/2 |
| u | 819.6 | Li | 812.6 ^a | 3s ² S ^o - 2p ² P ^o | 1/2 - 3/2; 1/2 - 1/2 |

Table S5. Deconvolution and peak assignment for the flame emission spectrum of JP10 – AlNPs taken at 17 ms (Fig. 2C).

| Peak /band | Peak wavelength / band center (nm) ^{a)} | Carrier | Reference wavelength (nm) | Transition | Branch; spin-orbit components; vibrational quantum numbers: (v', v'') or (v ₁ ', v ₂ ', v ₃ ') - (v ₁ '', v ₂ '', v ₃ '') |
|------------|--|----------------|---------------------------|---|---|
| a | 291.7 | Na | 285.3 ^a | 5p ² P ^o - 3s ² S | 3/2 - 1/2; 1/2 - 1/2 |
| b | 309.5 | OH | 309.9 ^b | A ² Σ ⁺ - X ² Π | (0-0), (1-1) |
| c | 436.6 | C ₂ | 435.4 ^b | d ³ Π _g - a ³ Π _u | (2-0), (3-1) |
| d | 588.5 | Na | 589.0 ^a | 3p ² P ^o - 3s ² S | 3/2 - 1/2; 1/2 - 1/2 |
| e | 670.3 | Li | 670.8 ^a | 2p ² P ^o - 2s ² S | 3/2 - 1/2; 1/2 - 1/2 |

Table S6. Deconvolution and peak assignment for the flame emission spectrum of JP10 – TiAlB RMNPs taken at 0 ms (Fig. 3A).

| Peak /band | Peak wavelength / band center (nm) ^{a)} | Carrier | Reference wavelength (nm) | Transition | Branch; spin-orbit components; vibrational quantum numbers: (v', v'') or (v ₁ ', v ₂ ', v ₃ ') - (v ₁ '', v ₂ '', v ₃ '') |
|------------|--|---------|---------------------------|--|--|
| a | 590.2 | Na | 589.0 ^a | 3p ² P ^o - 3s ² S | 3/2 - 1/2; 1/2 - 1/2 |
| b | 671.1 | Li | 670.8 ^a | 2p ² P ^o - 2s ² S | 3/2 - 1/2; 1/2 - 1/2 |
| c | 675.5 | Li | 670.8 ^a | 2p ² P ^o - 2s ² S | 3/2 - 1/2; 1/2 - 1/2 |
| d | 769.2 | K | 766.5 ^a | 4p ² P ^o - 4s ² S | 3/2 - 1/2; 1/2 - 1/2 |

Table S7. Deconvolution and peak assignment for the flame emission spectrum of JP10 – TiAlB RMNPs taken at 2 ms (Fig. 3B).

| Peak /band | Peak wavelength / band center (nm) ^{a)} | Carrier | Reference wavelength (nm) | Transition | Branch; spin-orbit components; vibrational quantum numbers: (v', v'') or (v ₁ ', v ₂ ', v ₃ ') - (v ₁ '', v ₂ '', v ₃ '') |
|------------|--|-----------------|---------------------------|---|---|
| a | 308.6 | OH | 309.9 ^b | A ² Σ ⁺ - X ² Π | (0-0), (1-1) |
| b | 314.9 | OH | 314.5 ^b | A ² Σ ⁺ - X ² Π | (2-2), (3-3) |
| c | 446.8 | BO ₂ | 448.8 ^c | A ² Π _u - X ² Π _g | (n,2,m)-(n-2,2,m), (n,3,0)-(n-1,3,m) |
| d | 454.7 | BO ₂ | 448.8 ^c | A ² Π _u - X ² Π _g | (n,2,m)-(n-2,2,m), (n,3,0)-(n-1,3,m) |
| e | 472.6 | BO ₂ | 469.6 ^c | A ² Π _u - X ² Π _g | (n,2,m)-(n-1,2,m), (n,1,m)-(n-2,1,m) |
| f | 493.8 | BO ₂ | 492.7 ^c | A ² Π _u - X ² Π _g | (n,0,m)-(n-2,0,m), (n,1,m)-(n-1,1,m) |
| g | 519.5 | BO ₂ | 518.1 ^c | A ² Π _u - X ² Π _g | (n,0,m)-(n-1,0,m), (n,1,m)-(n,1,m) |
| h | 526.1 | | | | |
| i | 548.1 | BO ₂ | 546.5 ^c | A ² Π _u - X ² Π _g | (n,0,m)-(n,0,m) |
| j | 556.5 | C ₂ | 559.8 ^b | d ³ Π _g - a ³ Π _u | (0-1), (1-2), (2-3) |
| k | 580.7 | BO ₂ | 581.2 ^c | A ² Π _u - X ² Π _g | (n,0,m)-(n+1,0,m), |
| l | 590.1 | Na | 589.0 ^a | 3p ² P ^o - 3s ² S | 3/2 - 1/2; 1/2 - 1/2 |
| m | 596.4 | Na | 589.6 ^a | 3p ² P ^o - 3s ² S | 3/2 - 1/2; 1/2 - 1/2 |
| n | 609.2 | Li | 610.4 ^a | 3d ² D - 2p ² P ^o | 5/2 - 3/2; 3/2 - 3/2; 3/2 - 1/2 |
| o | 624.0 | BO ₂ | 620.2 ^c | A ² Π _u - X ² Π _g | (n,0,m)-(n+2,0,m) |
| p | 642.1 | BO ₂ | 644.2 ^c | A ² Π _u - X ² Π _g | (n,0,m)-(n+3,0,m) |
| q | 673.1 | Li | 670.8 ^a | 2p ² P ^o - 2s ² S | 3/2 - 1/2; 1/2 - 1/2 |
| r | 675.6 | Li | 670.8 ^a | 2p ² P ^o - 2s ² S | 3/2 - 1/2; 1/2 - 1/2 |
| s | 691.2 | Li | 670.8 ^a | 2p ² P ^o - 2s ² S | 3/2 - 1/2; 1/2 - 1/2 |
| t | 713.0 | TiO | 713.6 ^b | A ³ Φ - X ³ Δ | (0-0), (1-1) |
| u | 723.5 | TiO | 713.6 ^b | A ³ Φ - X ³ Δ | (0-0), (1-1) |
| v | 768.2 | K | 769.9 ^a | 4p ² P ^o - 4s ² S | 3/2 - 1/2; 1/2 - 1/2 |
| w | 773.2 | K | 769.9 ^a | 4p ² P ^o - 4s ² S | 3/2 - 1/2; 1/2 - 1/2 |
| x | 783.5 | K | 769.9 ^a | 4p ² P ^o - 4s ² S | 3/2 - 1/2; 1/2 - 1/2 |

Table S8. Deconvolution and peak assignment for the flame emission spectrum of JP10 – TiAlB RMNPs taken at 29 ms (Fig. 3C).

| Peak /band | Peak wavelength / band center (nm) ^{a)} | Carrier | Reference wavelength (nm) | Transition | Branch; spin-orbit components; vibrational quantum numbers: (v', v'') or (v ₁ ', v ₂ ', v ₃ ') - (v ₁ '', v ₂ '', v ₃ '') |
|------------|--|---------|---------------------------|--|--|
| a | 589.3 | Na | 589.0 ^a | 3p ² P ^o - 3s ² S | 3/2 - 1/2; 1/2 - 1/2 |
| b | 594.2 | Na | 589.6 ^a | 3p ² P ^o - 3s ² S | 3/2 - 1/2; 1/2 - 1/2 |
| c | 671.0 | Li | 670.8 ^a | 2p ² P ^o - 2s ² S | 3/2 - 1/2; 1/2 - 1/2 |
| d | 674.0 | Li | 670.8 ^a | 2p ² P ^o - 2s ² S | 3/2 - 1/2; 1/2 - 1/2 |
| e | 677.2 | Li | 670.8 ^a | 2p ² P ^o - 2s ² S | 3/2 - 1/2; 1/2 - 1/2 |

^a reference ⁵

^b reference ⁶

^c reference ⁷

Movie S1 and S2. Levitated droplet during CO₂ laser irradiation. An envelope of aerosolized material develops around the droplet, which is then ignited. Eventually the burning droplet is de-trapped and falls from levitation.

Data S1: Basefunctions of various temperature dependent transitions extracted from Pgopher showing A) AlO, B) BO, C) BO₂, D) C₂, E) CH (A), F) CH (B), G) OH, and H) TiO.

References

- (1) Finn, M. T.; Chaloux, B. L.; Epshteyn, A. Exploring the Effects of Reaction Conditions on Morphology and Stability of Sonochemically Generated Ti–Al–B Fuel Powders. *Energy & Fuels* **2020**, *34* (9), 11373-11380. DOI: 10.1021/acs.energyfuels.0c01050.
- (2) *PGOPHER, a Program for Simulating Rotational Structure*; <http://pgopher.chm.bris.ac.uk> (accessed).
- (3) Rossum, G. v. Python reference manual. In *Department of Computer Science [CS]*, CWI: 1995.
- (4) Virtanen, P.; Gommers, R.; Oliphant, T. E.; Haberland, M.; Reddy, T.; Cournapeau, D.; Burovski, E.; Peterson, P.; Weckesser, W.; Bright, J.; et al. SciPy 1.0: fundamental algorithms for scientific computing in Python. *Nature Methods* **2020**, *17* (3), 261-272. DOI: 10.1038/s41592-019-0686-2.
- (5) Ralchenko, Y.; Kramida, A.; Reader, J. NIST atomic spectra database. *NIST Standard Reference Database* **2006**.
- (6) Huber, K.; Herzberg, G. IV. Constants of diatomic molecules. *Molecular Spectra and Molecular Structure*. New York, USA: Van Nostrand Reinhold Company **1979**.
- (7) Johns, J. W. C. THE ABSORPTION SPECTRUM OF BO₂. *Can. J. Phys.* **1961**, *39* (12), 1738-1768. DOI: 10.1139/p61-199.